Visible-light enabled C(Sp^3)–C(Sp^2) cross-electrophile coupling via synergistic halogen-atom transfer (XAT) and nickel catalysis

Girish Suresh Yedase, Avishek Kumar Jha and Veera Reddy Yatham*

School of Chemistry, Indian Institute of Science Education and Research, Thiruvananthapuram 695551, India.

*Email: reddy@iisertvm.ac.in

Table of contents

Optimization details:

General procedure for screening reactions: An oven-dried 10 mL glass vial was charged with Iodocyclo hexane (52.5 mg, 0.25 mmol), 4-bromomethyl benzoate (42.6 mg, 0.2 mmol), 4CzIPN (3.1 mg, 2 mol%), $^{t}Bu_3N$ (111.2 mg, 3.0 eq), $NiBr_2 \cdot L$ (10 mol%) and a PTFE-coated stirring bar and the glass vial was sealed with a PTFE septum. Under the positive pressure of argon, degassed solvent (2 mL) was added to the reaction vial. The reactions were placed in a temperature-controlled blue LED reactor (as shown in **Figure S1**) and the reaction mixture was irradiated with a 455 nm blue LED at 32 °C. After 40 h, a sample of this solution was analyzed by ^{1}H NMR using benzyl alcohol as the internal standard to determine the yield of the reaction.

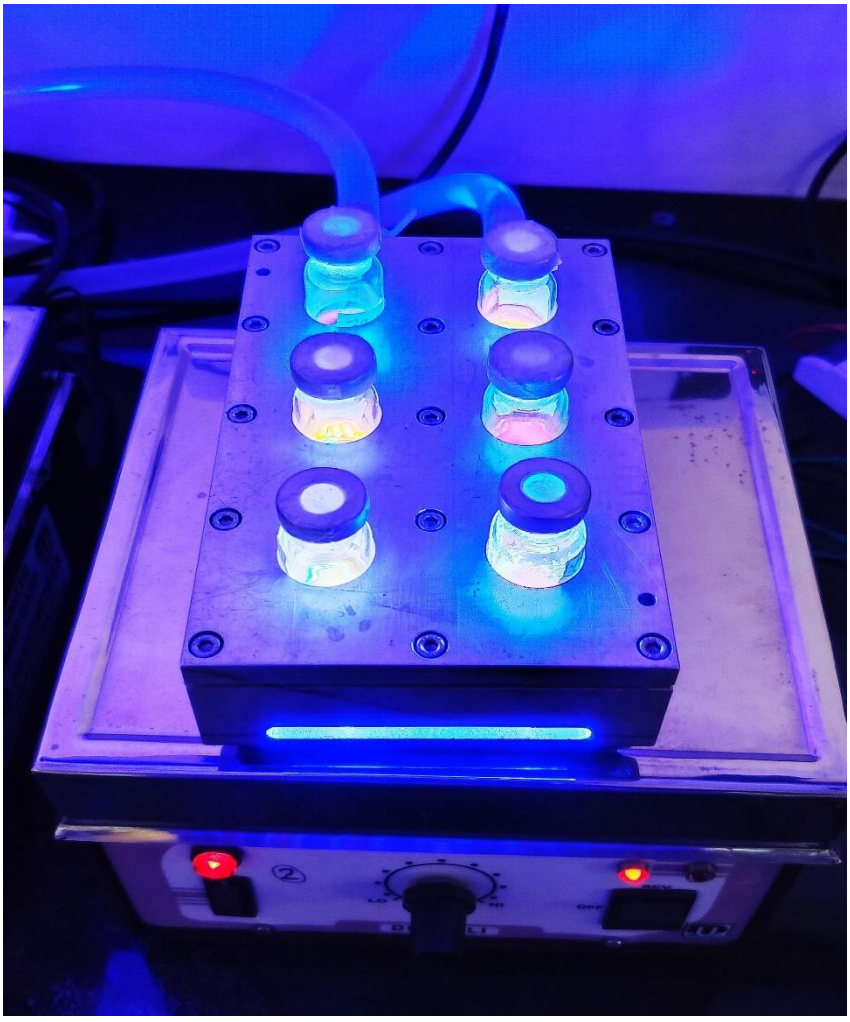

Figure S1: Blue LED reactor with magnetic stirring plate

Table S1: Optimization of the Reaction Conditions[a]

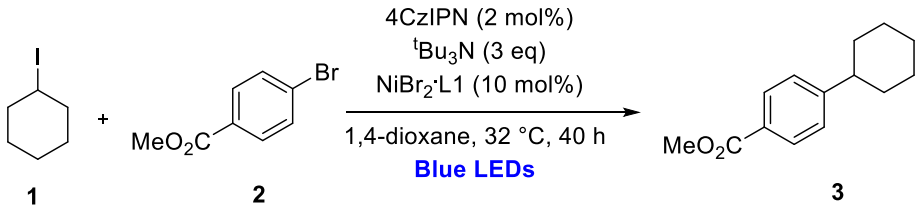

1 2 3

Entry	Deviation from standard conditions	3a(%)[b]
1	**None**	***70 (65%)***[c]
2	**$NiBr_2$·glyme** (10 mol%), **L1** (12 mol%) instead of **$NiBr_2$·L1** (10 mol%)	50-65
3	**$NiCl_2$·glyme** (10 mol%), **L1** (12 mol%) instead of **$NiBr_2$·L1** (10 mol%)	50
4	**NiI_2** (10 mol%), **L1** (12 mol%) instead of **$NiBr_2$·L1** (10 mol%)	5
5	**$Ni(OAc)_2·H_2O$**(10 mol%), **L1** (12 mol%) instead of **$NiBr_2$·L1** (10 mol%)	27
6	**$NiBr_2·H_2O$** (10 mol%), **L1** (12 mol%) instead of **$NiBr_2$·L1** (10 mol%)	30
7	**$NiBr_2$·L2** instead of **$NiBr_2$·L1**	*67*
8	**$NiBr_2$·L3** instead of **$NiBr_2$·L1**	*30*
9	**$NiBr_2$·L4** instead of **$NiBr_2$·L1**	*42*
10	**with 1 mol% of 4CzIPN**	*60*
11	**$NiBr_2·L_1$** (5 mol%)	*55*
12	$^tBu_3N$ (2 eq)	*56*
13	**Ir-I** instead of 4CzIPN	50
14	**Ir-II** instead of 4CzIPN	40
15	**9,10 Diphenyl Anthracene** instead of 4CzIPN	0
16	**Et_3N** instead of **$^tBu_3N$**	44
17	**DIPEA** instead of **$^tBu_3N$**	30
18	**2,2,6,6-Tetramethylpiperidine** instead of **$^tBu_3N$**	0
19	**1,2,2,6,6-Pentamethylpiperidine** instead of **$^tBu_3N$**	31
20	**DABCO** instead of **$^tBu_3N$**	0
21	**CH_3CN** instead of **1,4-dioxane**	54
22	**THF** instead of **1,4-dioxane**	64
23	**EtOAc** instead of **1,4-dioxane**	56
24	**DMF** instead of **1,4-dioxane**	28
25	**Tolune instead of 1,4-dioxane**	52
26	**without** $^tBu_3N$	0
27	**without** 4CzIPN	0
28	**without** $NiBr_2$·L1	0
29	**without** Blue Led's	0

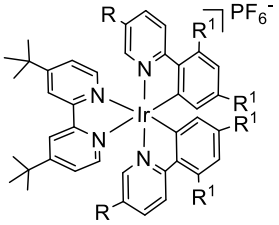

Ir-I, R = CF_3, R_1 = F
Ir-II, R = R_1 = H

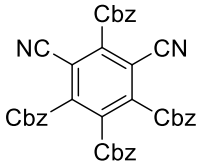

Cbz = Carbazole

4CzIPN

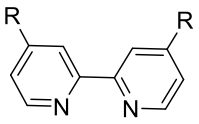

L1 = R = tBu
L2 = R= OMe
L3 = R = H

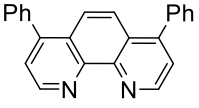

L4

[a]**1a** (0.25 mmol), **2a** (0.2 mmol), 4CzIPN (2 mol%), $^tBu_3N$ (3.0 eq), $NiBr_2$ L1 (10 mol%), 1,4-dioxane (2 ml) at 32 °C, 40 h [b] NMR yields using benzylalcohol as an internal standard. [c]Isolated yield.

X-ray Structure

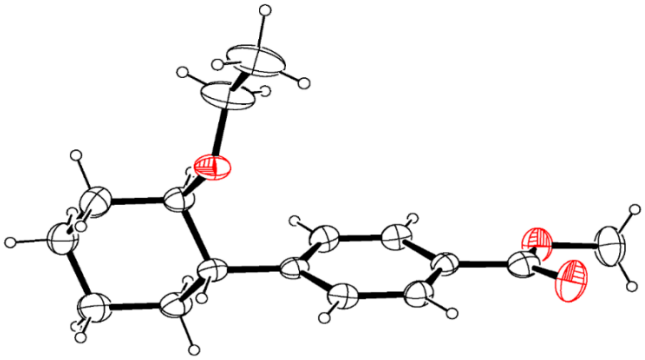

Figure S2: ORTEP of the X-ray crystal structure of **7** (trans). Thermal ellipsoids are drawn at a 20% probability level.

Crystals of **7** (trans) for X-ray analysis were obtained from slow evaporation of 1:1 Methanol and Ethyl acetate at room temperature over 5 days. X-ray diffraction data were collected on a Bruker Kappa Apex-II CCD diffractometer at 296 K.

Table S2. Crystal data and structure refinement for 7 (trans)

Empirical formula	C16 H22 O3	
Formula weight	262.33	
Temperature	296(2) K	
Wavelength	0.71073 Å	
Crystal system	Triclinic	
Space group	P -1	
Unit cell dimensions	a = 5.6173(18) Å	α= 95.098(10)°.
	b = 11.605(4) Å	β= 95.073(10)°.
	c = 11.772(4) Å	γ = 91.735(10)°.
Volume	760.8(4) $Å^3$	
Z	2	
Density (calculated)	1.145 Mg/m^3	
Absorption coefficient	0.078 mm^{-1}	
F(000)	284	
Crystal size	0.075 x 0.030 x 0.028 mm^3	
Theta range for data collection	2.592 to 24.999°.	
Index ranges	-6<=h<=6, -13<=k<=13, -13<=l<=13	
Reflections collected	17924	
Independent reflections	2674 [R(int) = 0.0853]	
Completeness to theta = 24.999°	99.9 %	
Absorption correction	Semi-empirical from equivalents	
Max. and min. transmission	0.997 and 0.994	
Refinement method	Full-matrix least-squares on F^2	
Data / restraints / parameters	2674 / 0 / 175	
Goodness-of-fit on F^2	0.997	
Final R indices [I>2sigma(I)]	R1 = 0.0526, wR2 = 0.1130	
R indices (all data)	R1 = 0.1657, wR2 = 0.1631	
Extinction coefficient	0.024(5)	
Largest diff. peak and hole	0.135 and -0.147 $e.Å^{-3}$	

Mechanistic Studies:

ON/OFF experiment:

An oven-dried 10 mL glass vial was charged with iodocyclohexane (52.5mg, 0.25 mmol), methyl 4-bromobenzoate (43 mg, 0.2 mmol), 4CzIPN (3.1 mg, 2 mol%), nBu3N (111.2 mg, 0.6 mmol), $NiBr_2$.L1 (9.7 mg, 10 mol%), benzyl benzoate (0.2 mmol, internal standard), a PTFE-coated stirring bar and the glass vial was sealed with a PTFE septum. Under positive pressure of argon, degassed 1,4-dioxane (2 mL) was added to the reaction vial. The reactions were placed in a temperature-controlled blue LED reactor (as shown in Figure 1) and the reaction mixture was irradiated with a 455 nm blue LED. To monitor the reaction progress, a small aliquot was removed after specific time intervals and concentrated under reduced pressure, and analyzed by ^{1}H NMR to determine the product yield.

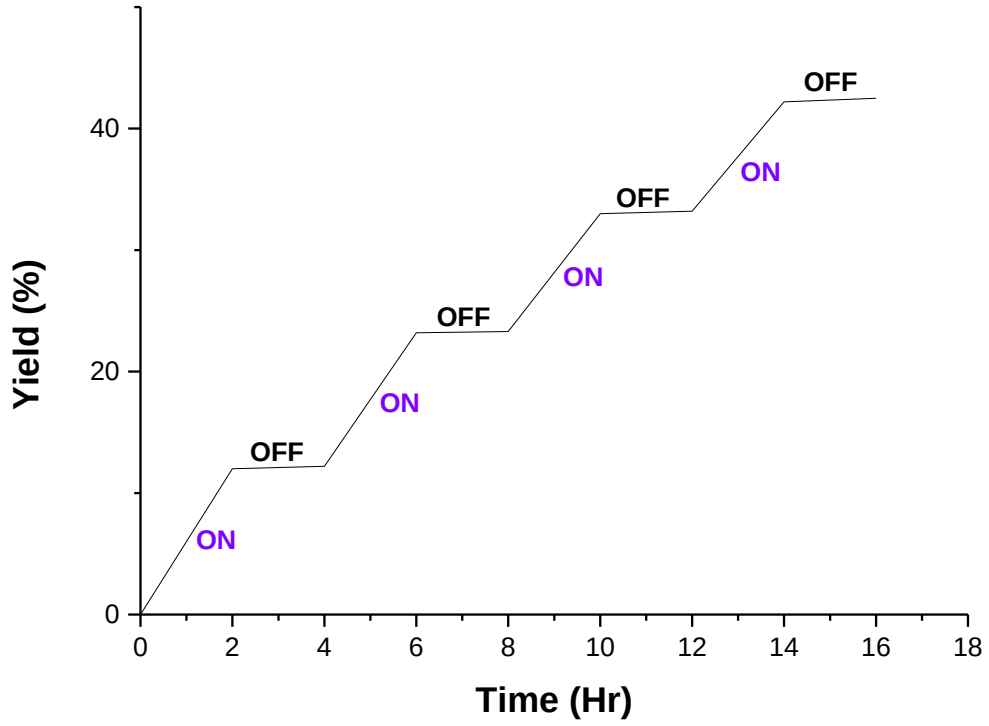

Figure S3. ON/OFF experiment (The reaction profile during alternating irradiation shows that the reaction does only proceed in the presence of light).

Luminescence quenching experiments:

Fluorescence spectra were collected on Fluorolog Horiba Jobin Yvon spectrofluorimeter. Samples for the quenching experiments were prepared in a 4 mL glass cuvette with a septum screw cap. 4CzIPN was irradiated at 470 nm and the emission intensity at 570 nm was observed. In a typical experiment, the emission spectrum of a 0.00025 M solution of 4CzIPN in 1,4-dioxane was collected in presence of different quenchers.

Tributylamine: The Increasing amount of tributylamine (2.8 mM to 14 mM) were added to a solution of the photocatalyst 4CzIPN in 1,4-dioxane (0.00025 M).

As shown below, a significant decrease of 4CzIPN luminescence was observed in presence of tributylamine, suggesting that the mechanism might operate via a canonical photoredox cycle consisting of a reductive quenching with tributylamine.

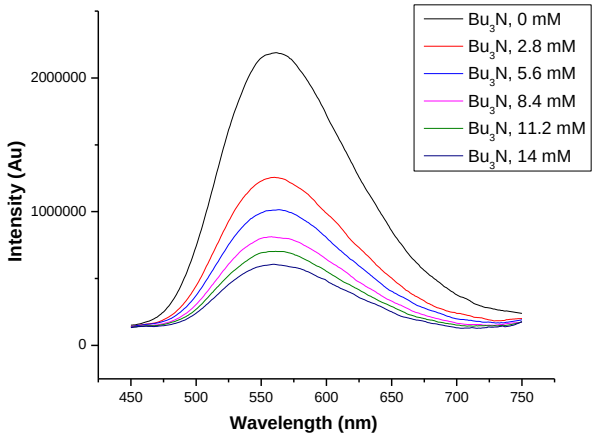

Figure S4. Luminescence quenching experiment of Bu_3N in presence of 4CzIPN

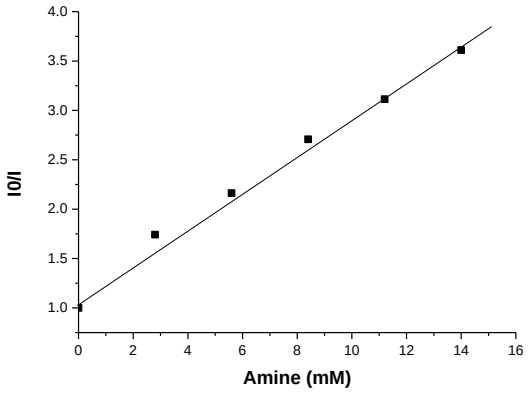

Figure S5. Stern Volmer plot of $^{n}Bu_3N$ in presence of 4CzIPN

The Increasing amount of substrate 4-bromomethyl benzoate and iodo cyclohexane were added directly to a solution of the photocatalyst (4CzIPN) in 1,4-dioxane (0.00025 M). In both cases, negligible 4CzIPN luminescence was observed.

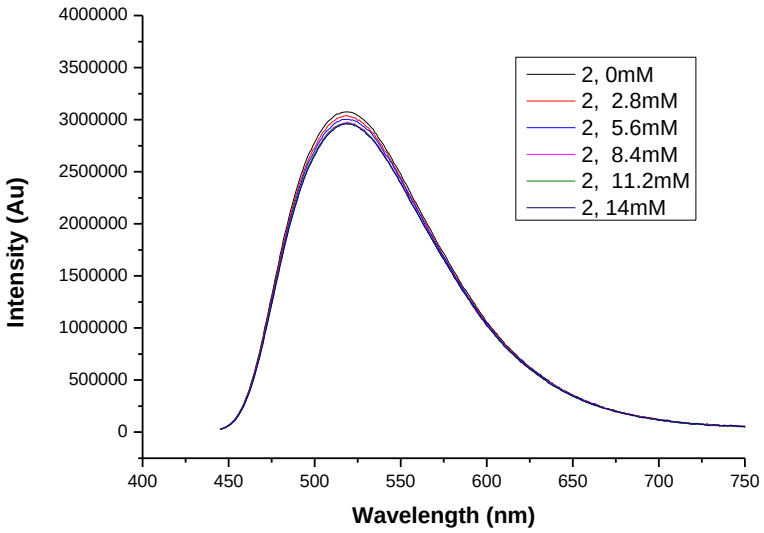

Figure S6. Luminescence quenching experiment of Methyl 4-bromobenzoate (**2)** in presence of 4CzIPN

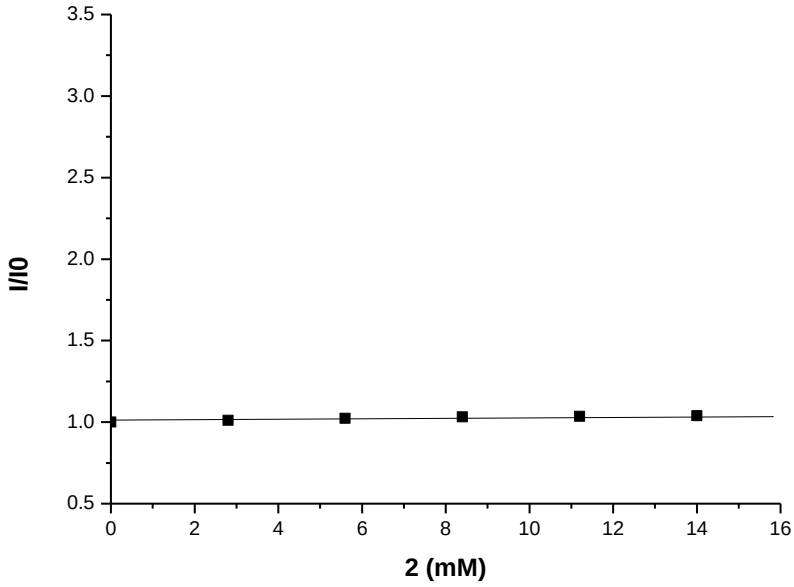

Figure S7. Stern Volmer plot of Methyl 4-bromobenzoate (**2**) in presence of 4CzIPN

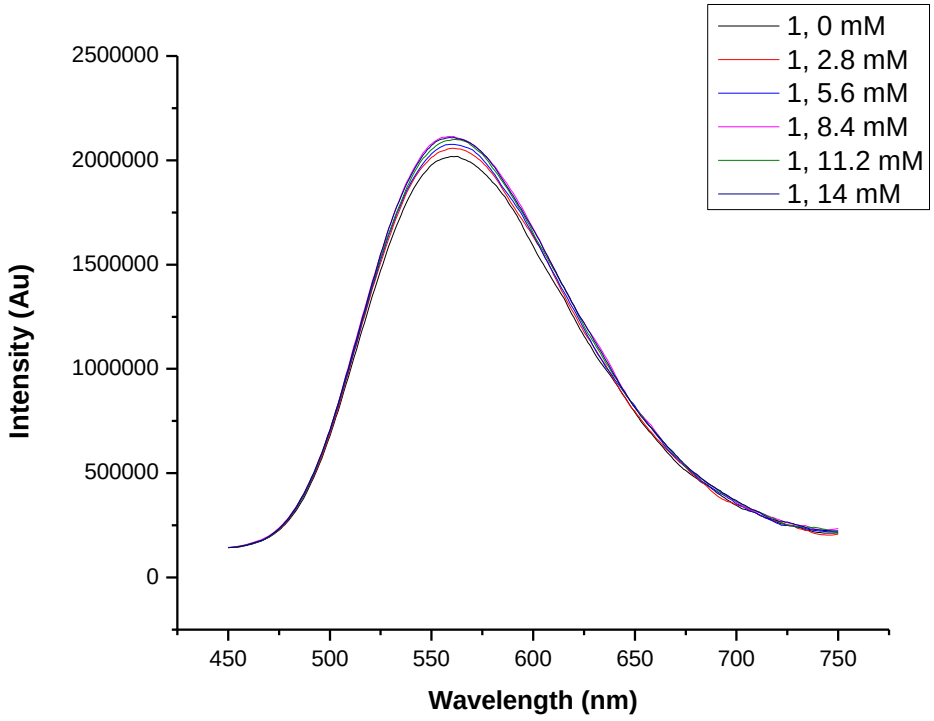

Figure S8. Luminescence quenching experiment of iodo cyclohexane (**1**) in presence of 4CzIPN

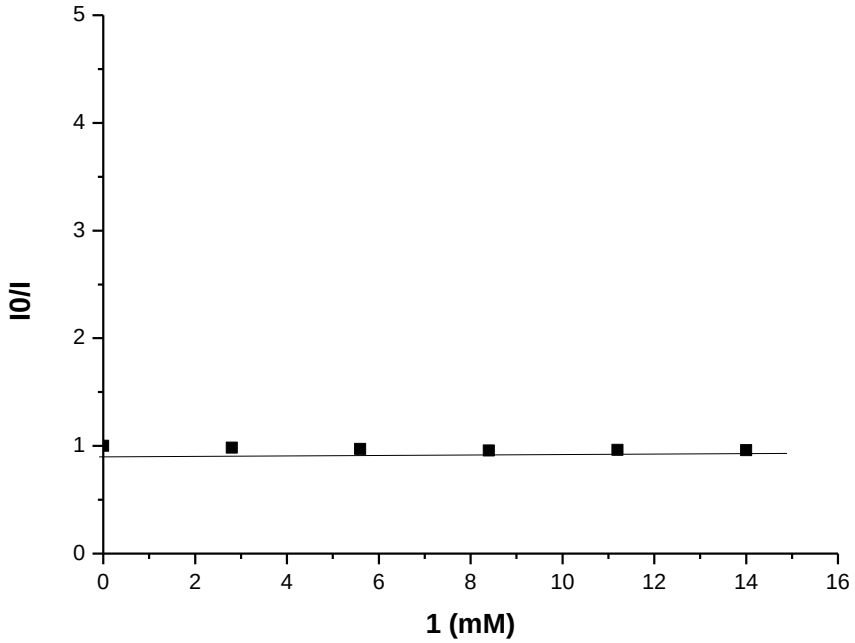

Figure S9. Stern Volmer plot of Iodo cyclohexane (**1)** in presence of 4CzIPN

2, 2,6,6-Tetramethylpiperidine (TMP) and DABCO: The Increasing amount of TMP and DABCO (2.8 mM to 14 mM) were added to a solution of the photocatalyst 4CzIPN in 1,4-dioxane (0.00025 M). As shown below, a significant decrease of 4CzIPN luminescence was observed in presence of tributylamine, suggesting the generation of the amino radical cation.

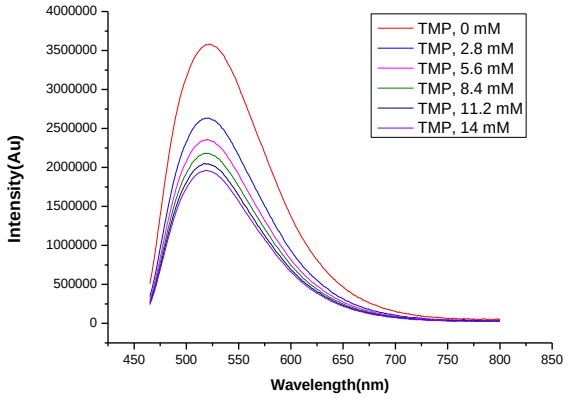

Figure S10. Luminescence quenching experiment of TMP in presence of 4CzIPN

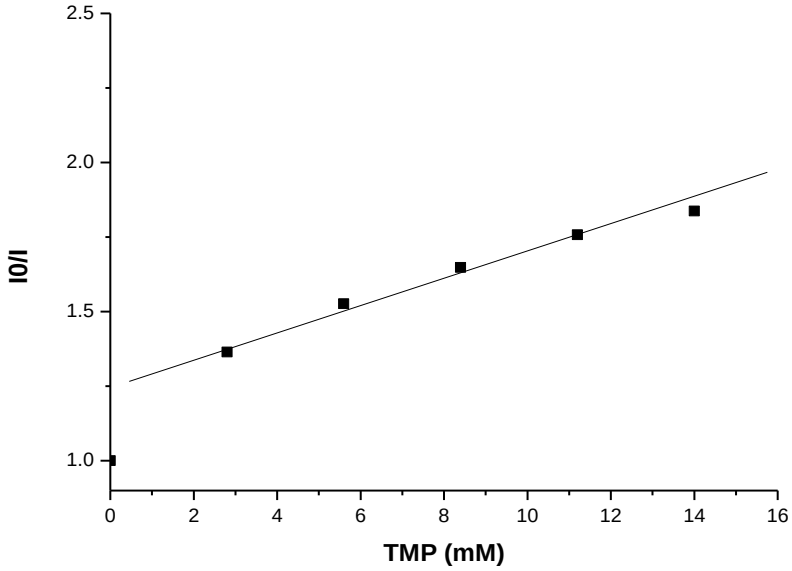

Figure S11. Stern Volmer plot of TMP in presence of 4CzIPN

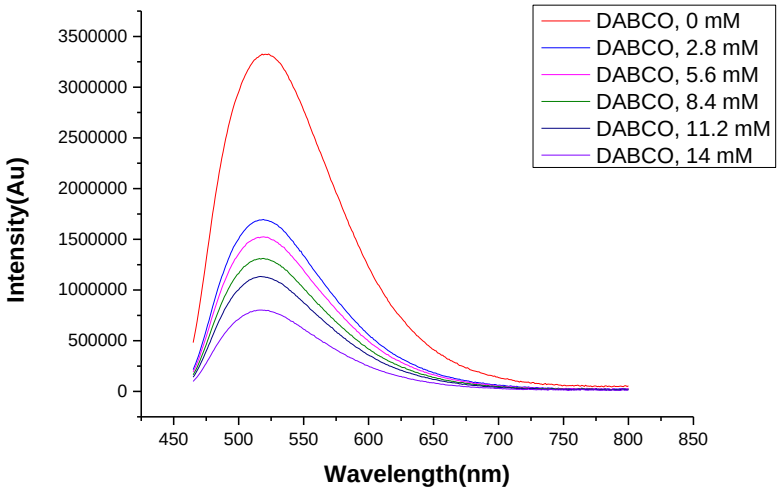

Figure S12. Luminescence quenching experiment of DABCO in presence of 4CzIPN

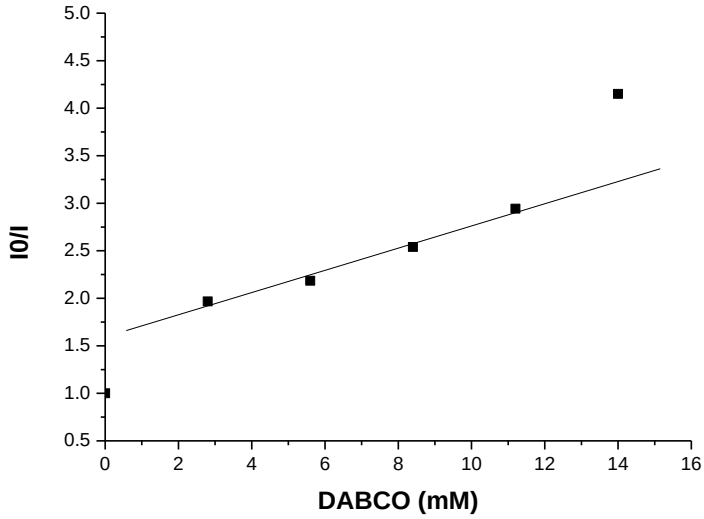

Figure S13. Luminescence quenching experiment of DABCO in presence of 4CzIPN

Radical Trapping Experiment:

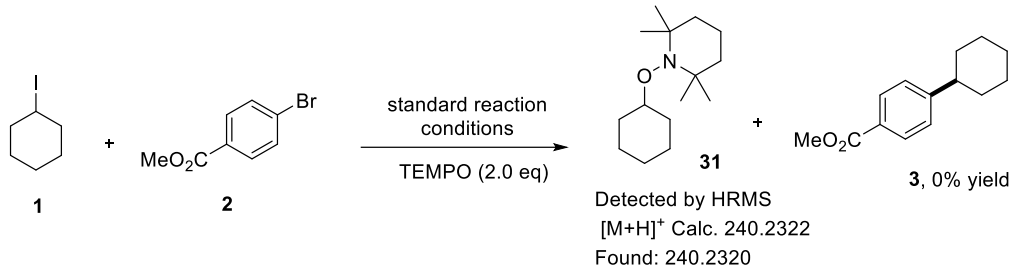

An oven-dried 10 mL glass vial was charged with iodocyclohexane (52.5 mg, 0.25 mmol), methyl 4-bromobenzoate (43 mg, 0.2 mmol), 4CzIPN (3.1 mg, 2 mol%), nBu_3N (111.2 mg, 0.6 mmol), $NiBr_2$.L1 (9.7 mg, 10 mol%), TEMPO (62.4 mg, 0.4 mmol, 2.0 equiv), a PTFE-coated stirring bar and the glass vial was sealed with a PTFE septum. Under positive pressure of argon, degassed 1,4-dioxane (2 mL) was added to the reaction vial. The reactions were placed in a temperature-controlled blue LED reactor (as shown in **Figure 1**) and the reaction mixture was irradiated with a 455 nm blue LED. After 40 h, a sample of this solution was analyzed by HRMS observed 1-(cyclohexyloxy)-2,2,6,6-tetramethyl piperidine (**30**).

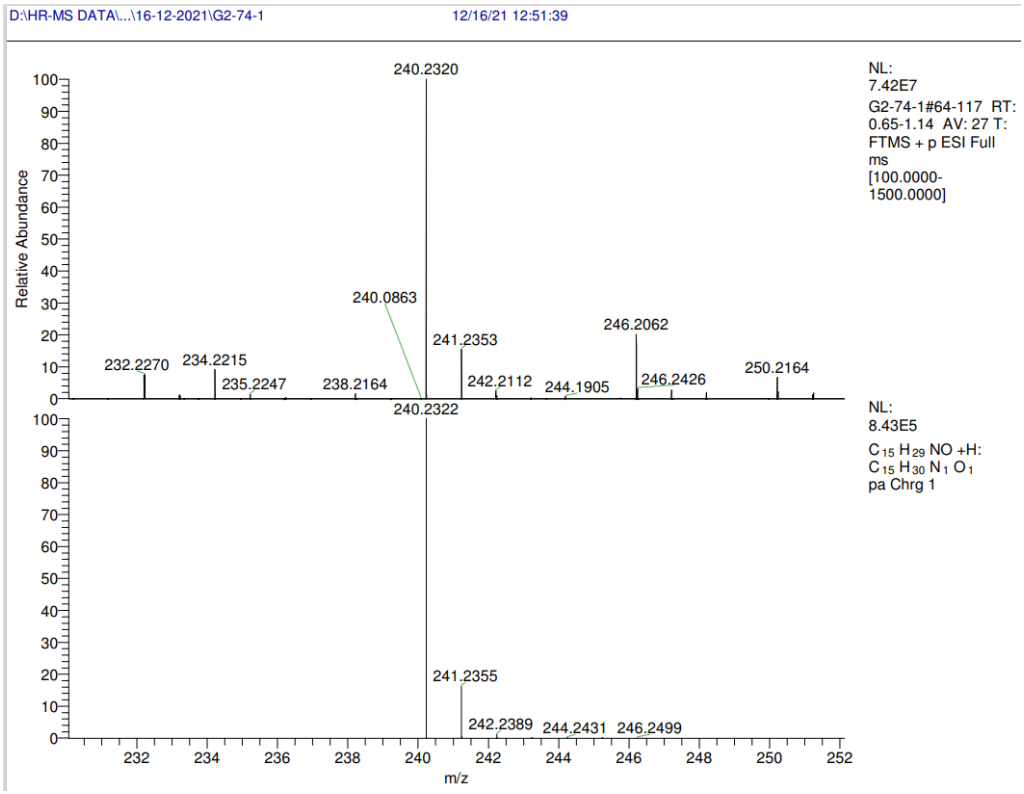

Figure S14. HRMS{ESI/Q-ORBITRAP} spectrum of the reaction mixture

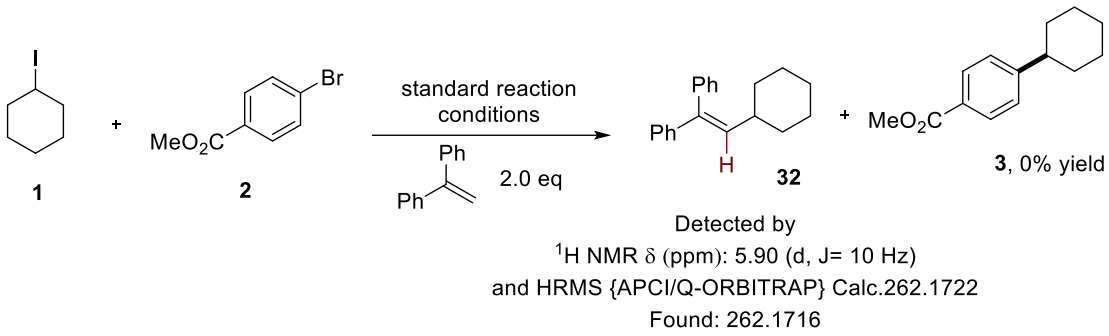

An oven-dried 10 mL glass vial was charged with iodocyclohexane (52.5 mg, 0.25 mmol), methyl 4-bromobenzoate (43 mg, 0.2 mmol), 4CzIPN (3.1 mg, 2 mol%), nBu_3N (111.2 mg, 0.6 mmol), $NiBr_2$.L1 (9.7 mg, 10 mol%), ethene-1,1-diyldibenzene (79.2 mg, 0.4 mmol, 2.0 equiv), a PTFE-coated stirring bar and the glass vial was sealed with a PTFE septum. Under positive pressure of argon, degassed 1,4-dioxane (2 mL) was added to the reaction vial. The reactions were placed in a temperature-controlled blue LED reactor (as shown in **Figure 1**) and the reaction mixture was irradiated with a 455 nm blue LED. After 40 h, a sample of this solution was analyzed by ^{1}H NMR using benzyl alcohol as the internal standard observed (2-cyclohexylethene-1,1-diyl)dibenzene (**31**) in 20% yield.

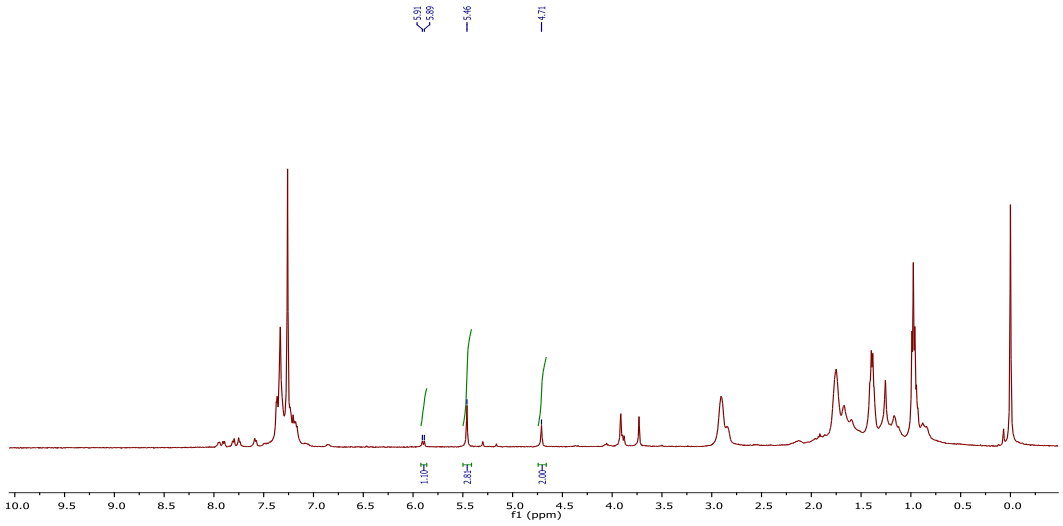

Figure S15. ^{1}H NMR spectrum of the crude reaction mixture in presence of benzyl alcohol as internal standard.

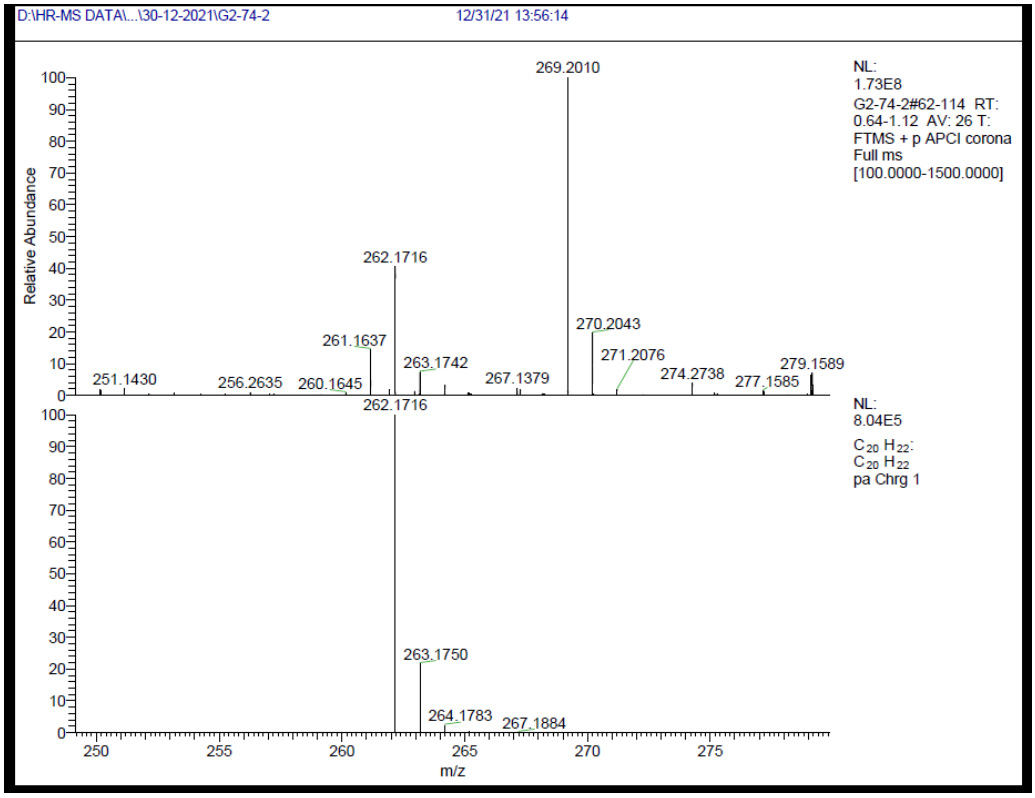

Figure S16. HRMS{APCI/Q-ORBITRAP} spectrum of the reaction mixture

Employing different haloalkanes and haloarenes

Reaction with Methyl 4-bromobenzoate with different Iodoalkanes afford the products as shown below. In TLC these products show the same polarity with respect to the 4CzIPN, separation is not possible.

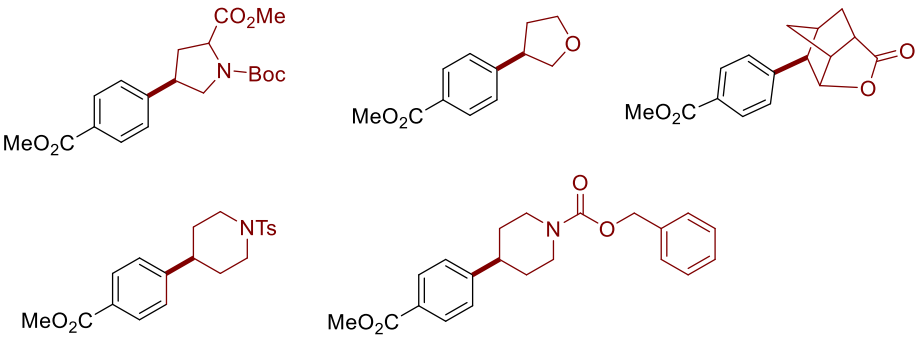

Figure S17. Cross-coupling products that are difficult to isolate through column chromatography.

Haloalkanes and aryl bromides/chlorides do not work in our catalysis:

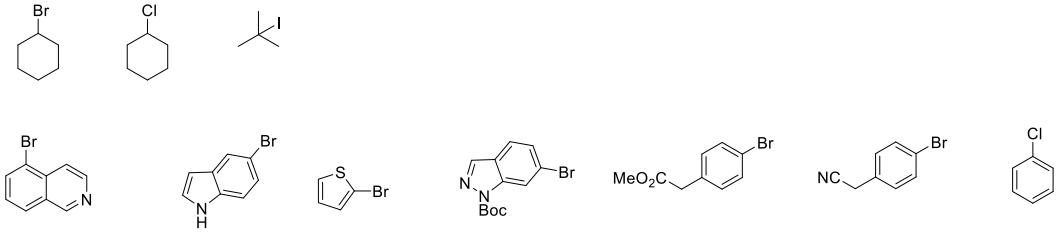

Figure S18. List of the substrates that did not work in our catalysis

NMR data

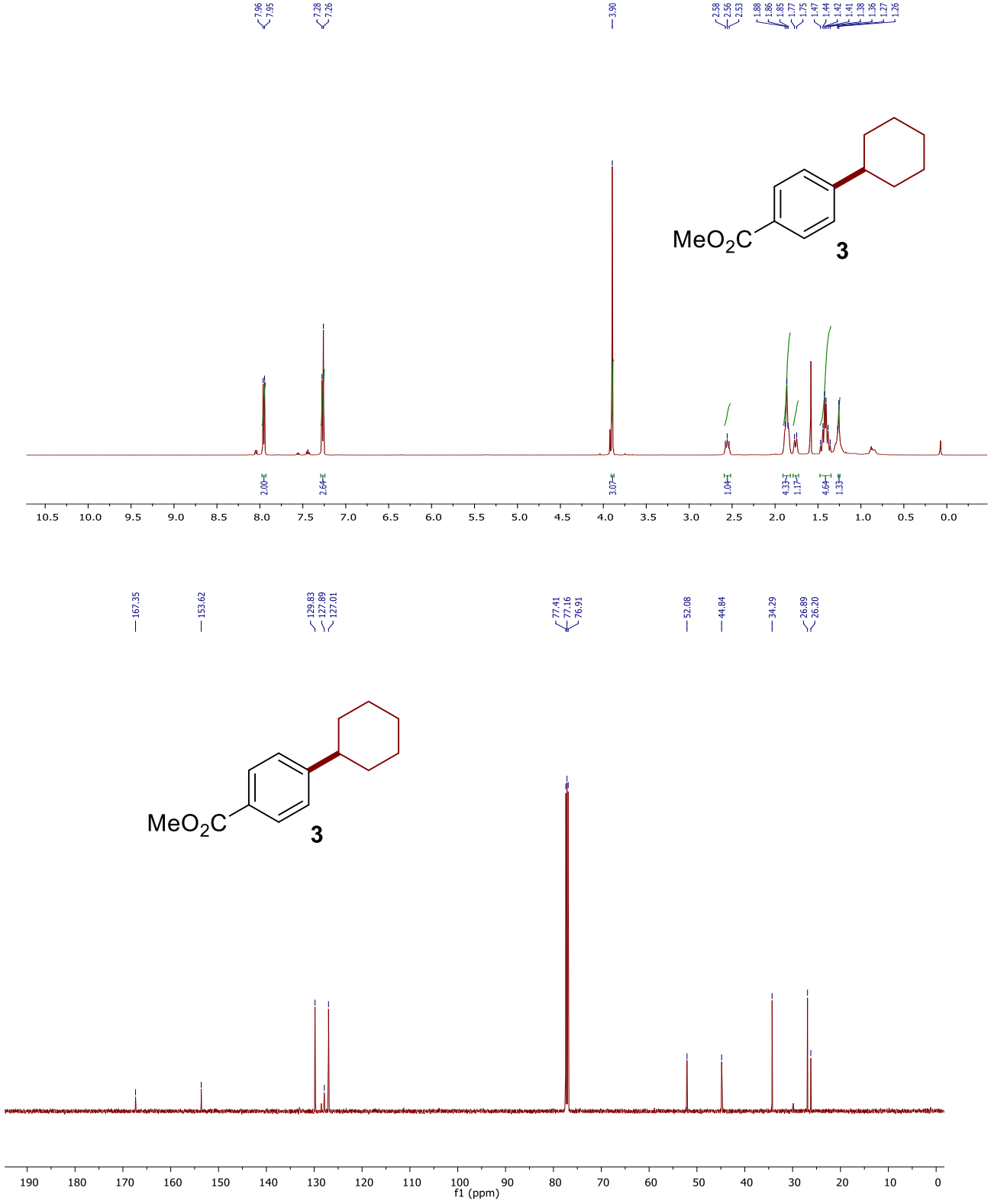

Figure S19. ^{1}H NMR (500 MHz, top) and ^{13}C {1 H} NMR (125 MHz, bottom) Spectra of **3** in $CDCl_3$ at 298K.

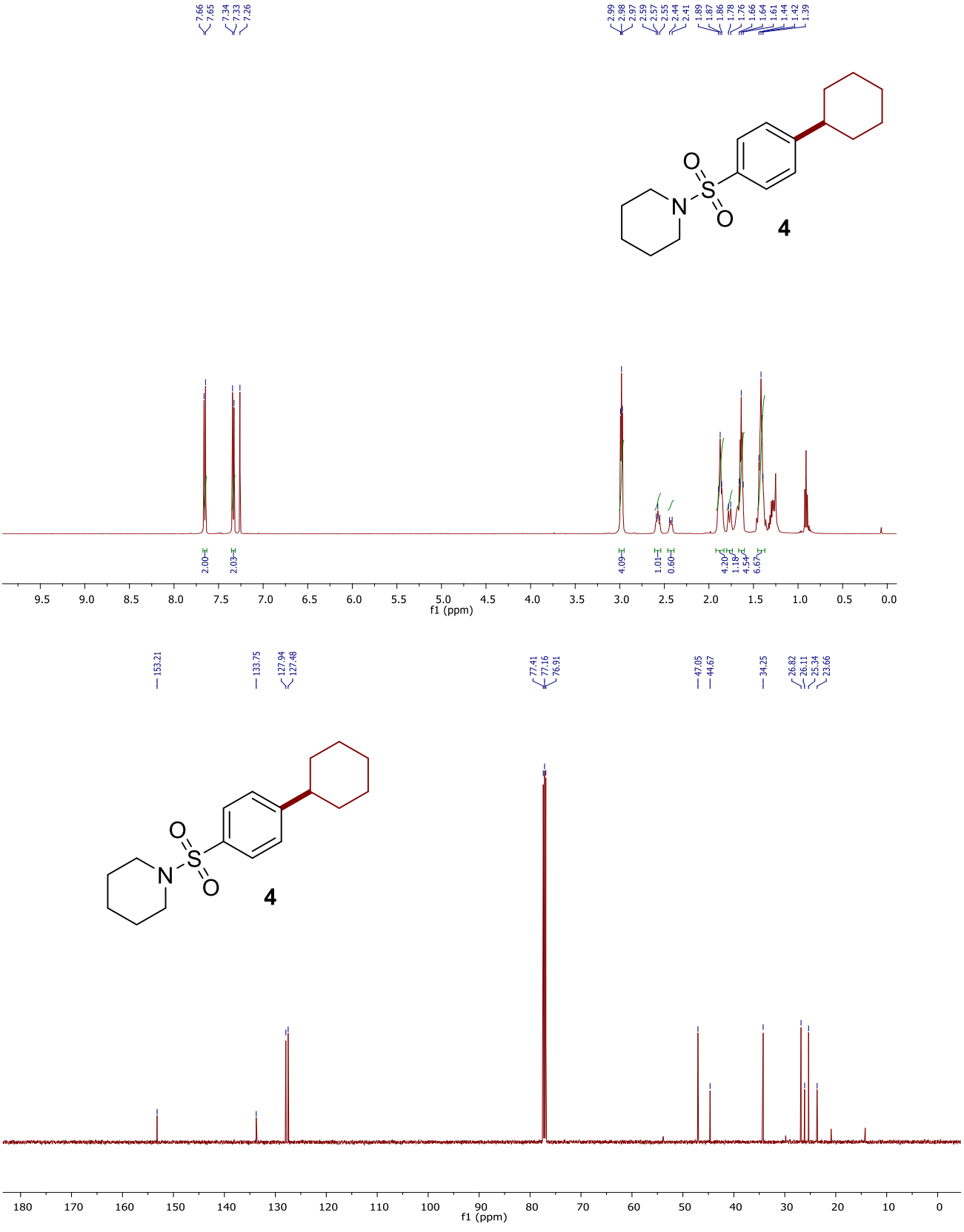

Figure S20. ^{1}H NMR (500 MHz, top) and ^{13}C {1 H} NMR (125 MHz, bottom) Spectra of **4** in $CDCl_3$ at 298K.

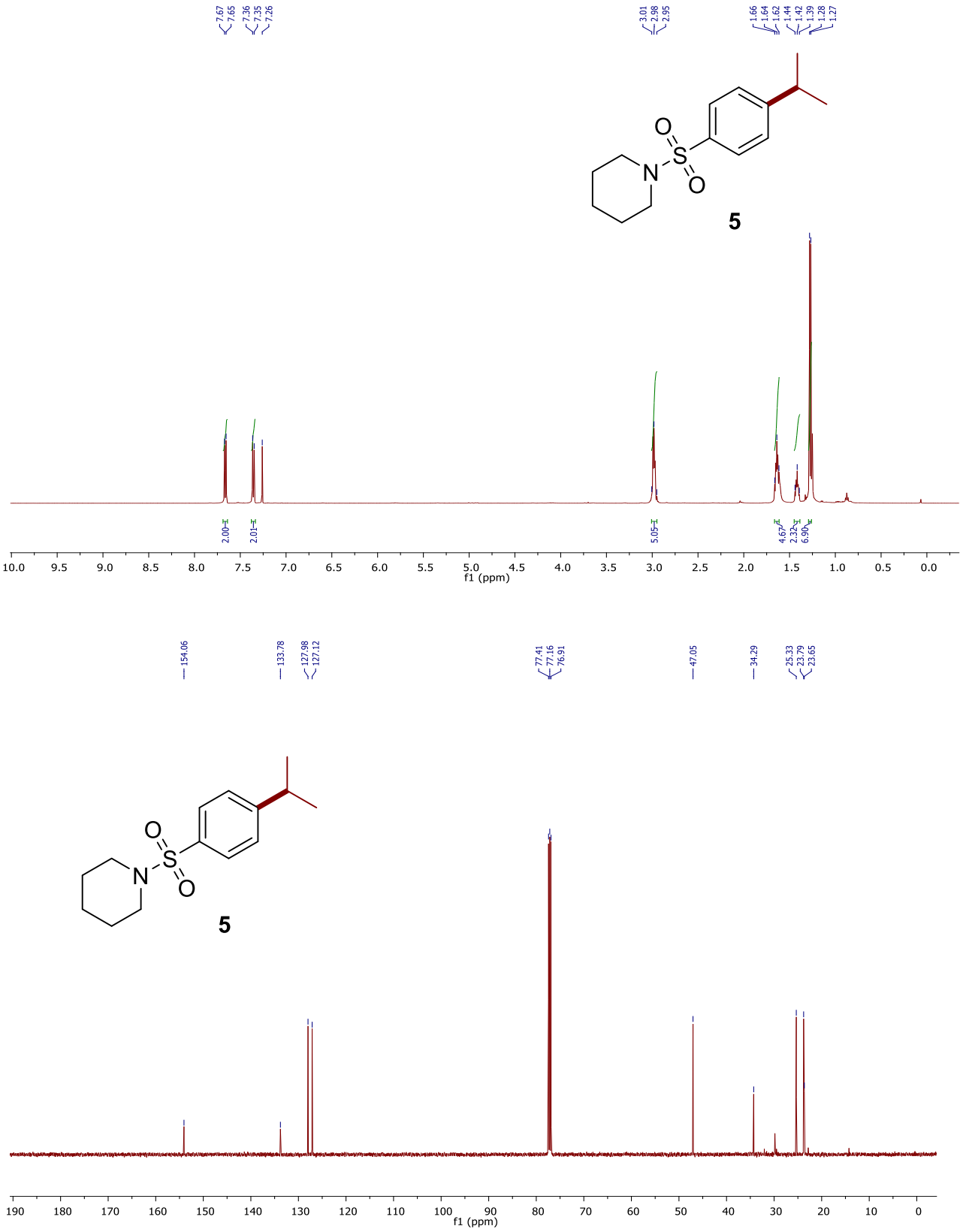

Figure S21. ^{1}H NMR (500 MHz, top) and ^{13}C {1 H} NMR (125 MHz, bottom) Spectra of **5** in $CDCl_3$ at 298K.

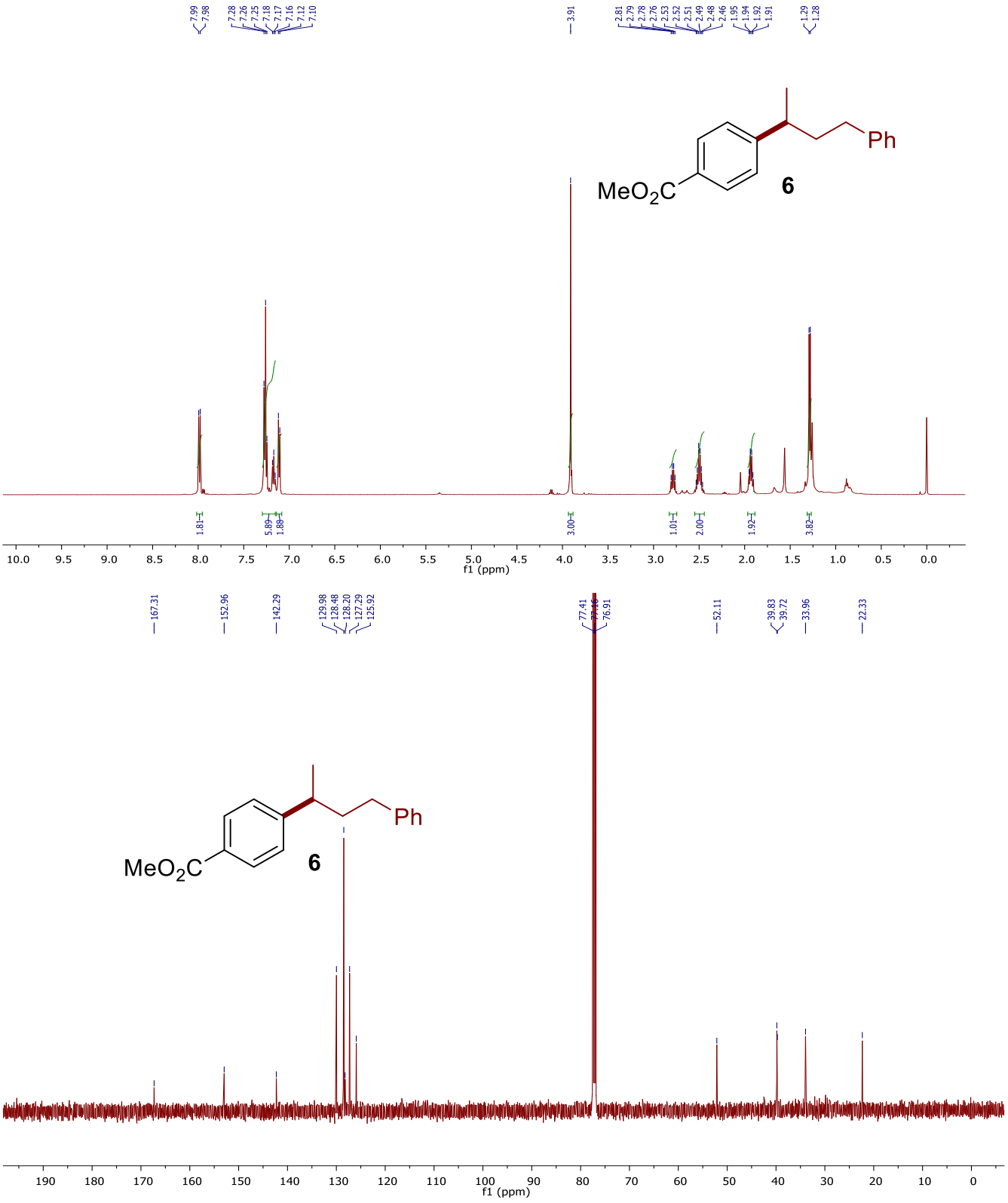

Figure S22. ^{1}H NMR (500 MHz, top) and ^{13}C {1 H} NMR (125 MHz, bottom) Spectra of **6** in $CDCl_3$ at 298K.

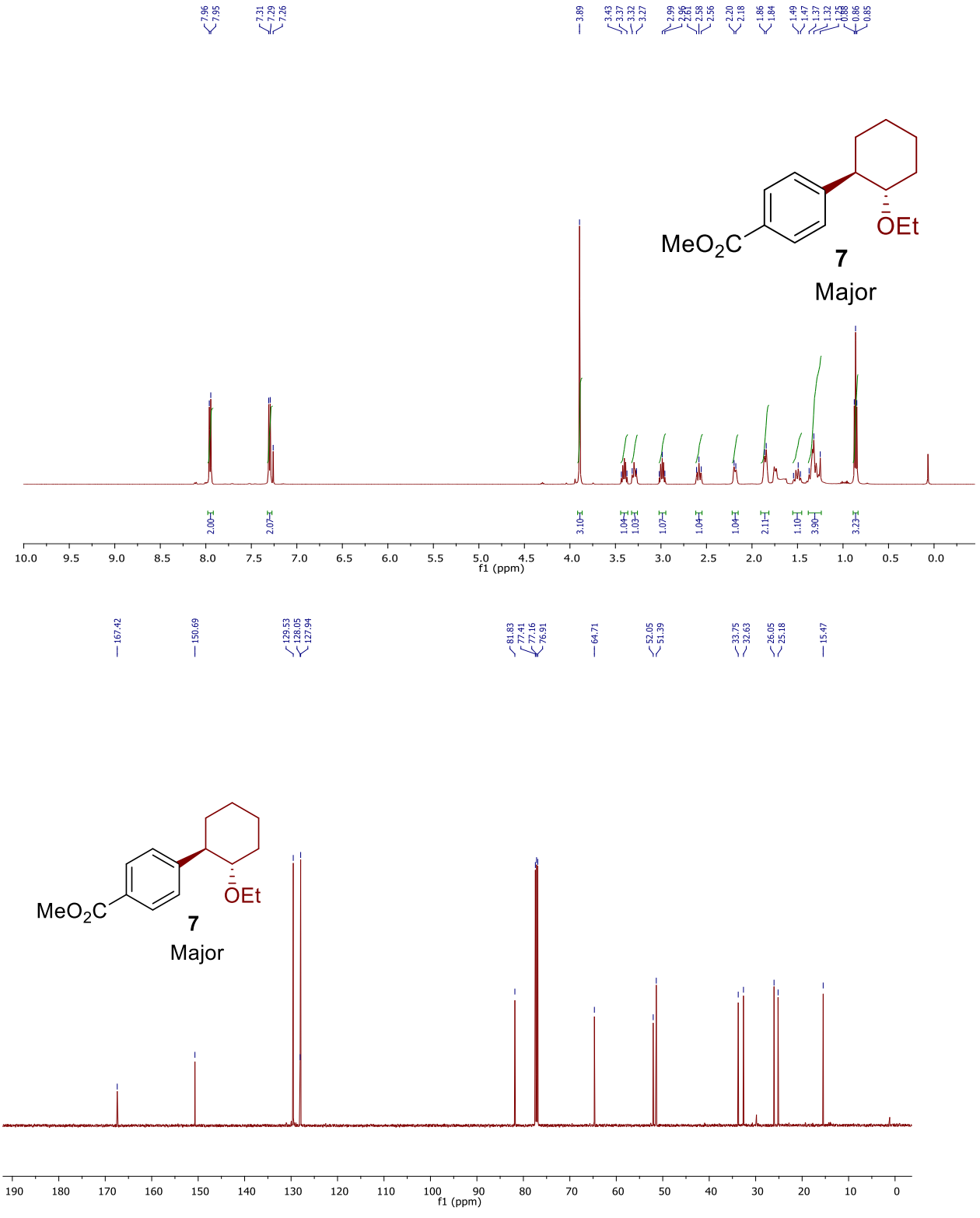

Figure S23. ^{1}H NMR (500 MHz, top) and ^{13}C {1 H} NMR (125 MHz, bottom) Spectra of **7** (major) in $CDCl_3$ at 298K.

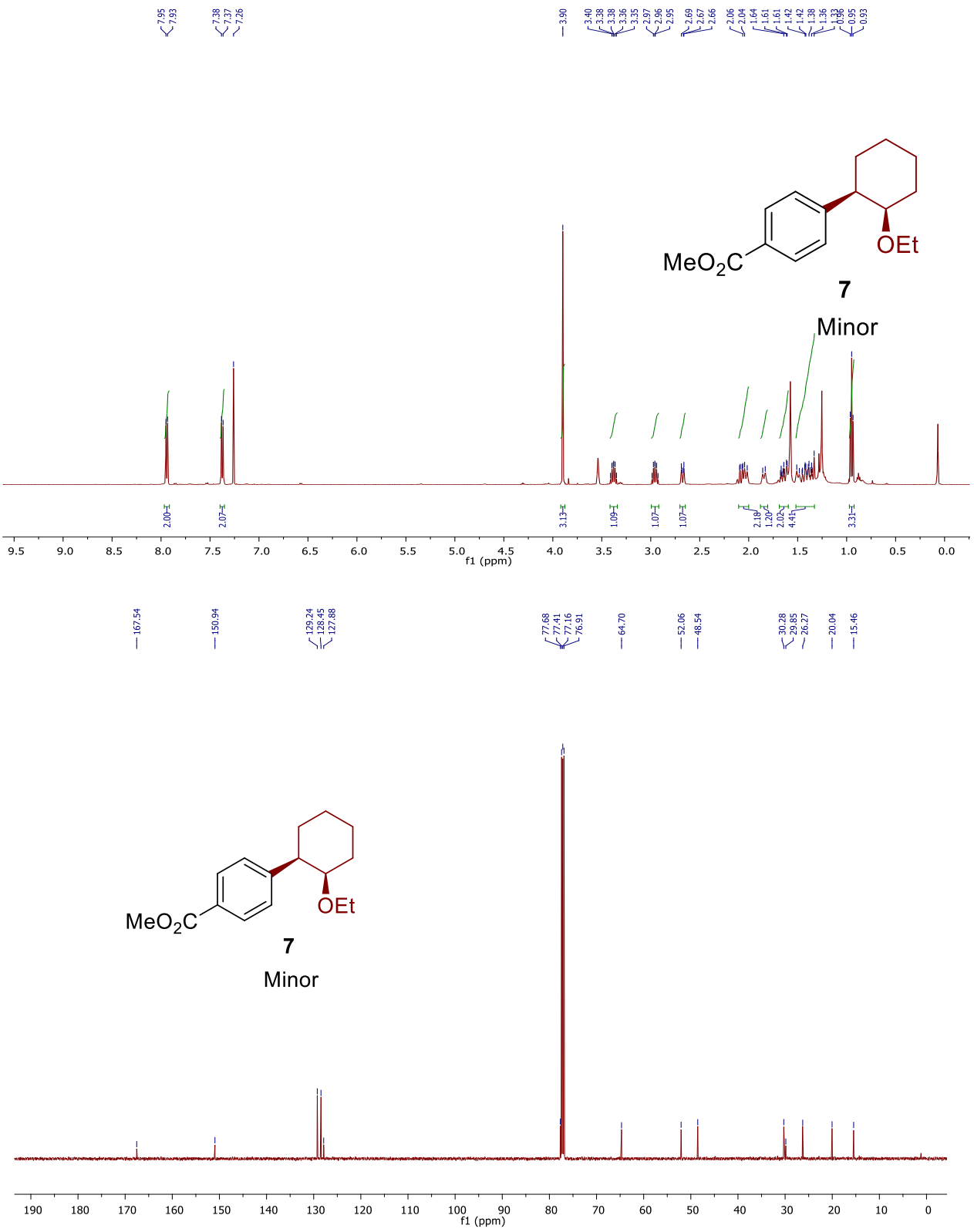

Figure S24. ^{1}H NMR (500 MHz, top) and ^{13}C {1 H} NMR (125 MHz, bottom) Spectra of **7** (minor) in $CDCl_3$ at 298K.

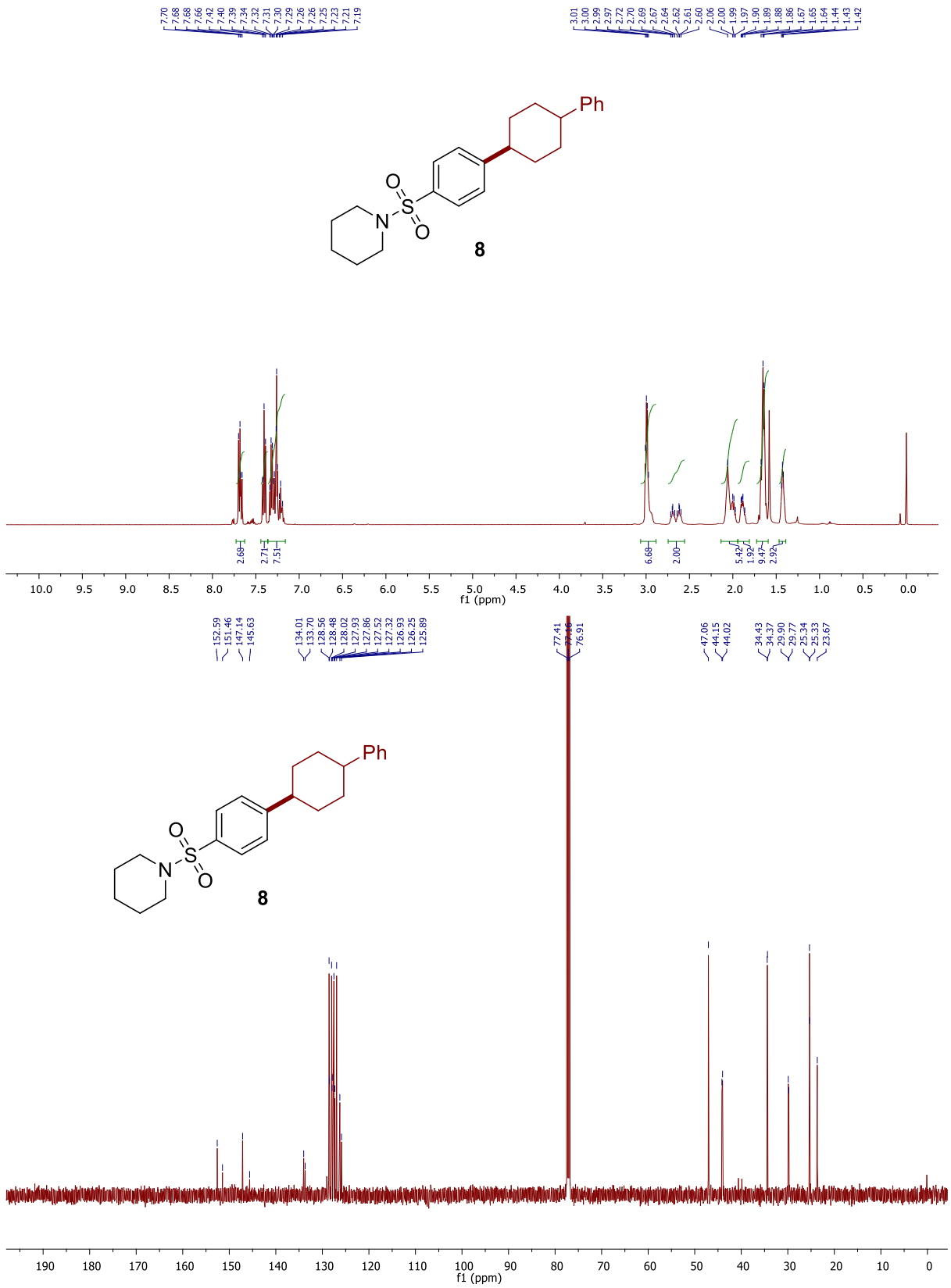

Figure S25. ^{1}H NMR (500 MHz, top) and ^{13}C {1 H} NMR (125 MHz, bottom) Spectra of **8** in $CDCl_3$ at 298K.

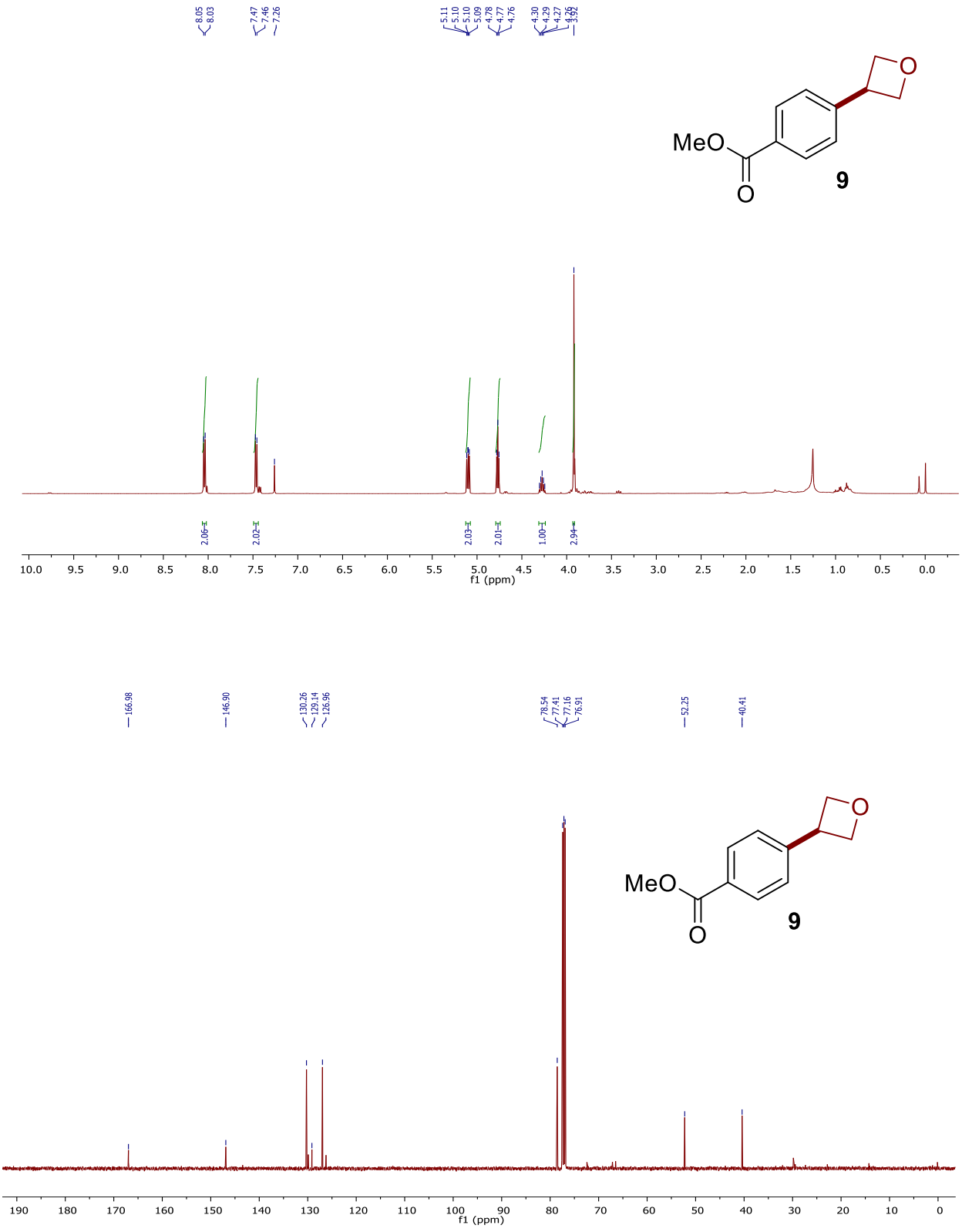

Figure S26. ^{1}H NMR (500 MHz, top) and ^{13}C {1 H} NMR (125 MHz, bottom) Spectra of **9** in $CDCl_3$ at 298K.

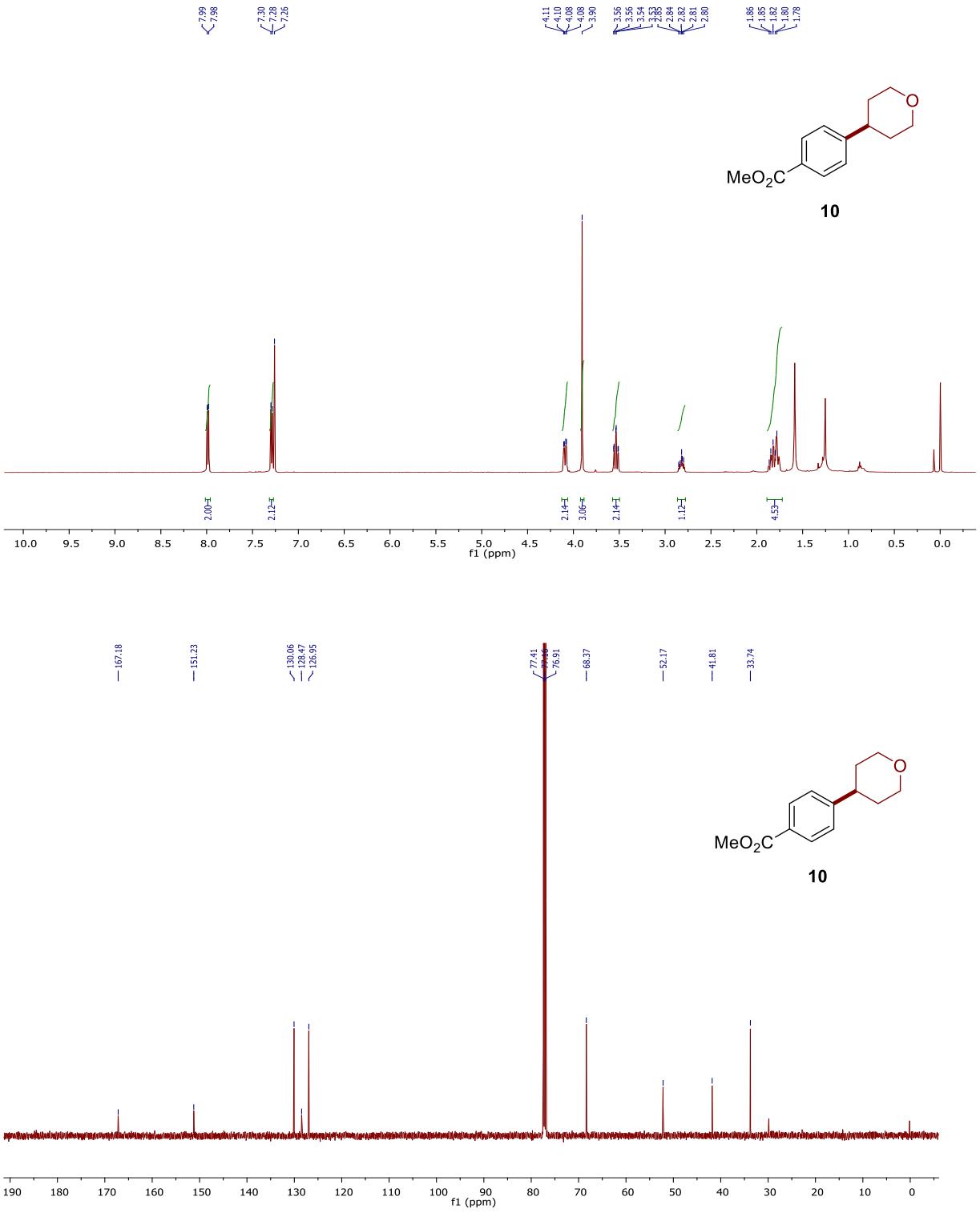

Figure S27. ^{1}H NMR (500 MHz, top) and ^{13}C {1 H} NMR (125 MHz, bottom) Spectra of **10** in $CDCl_3$ at 298K.

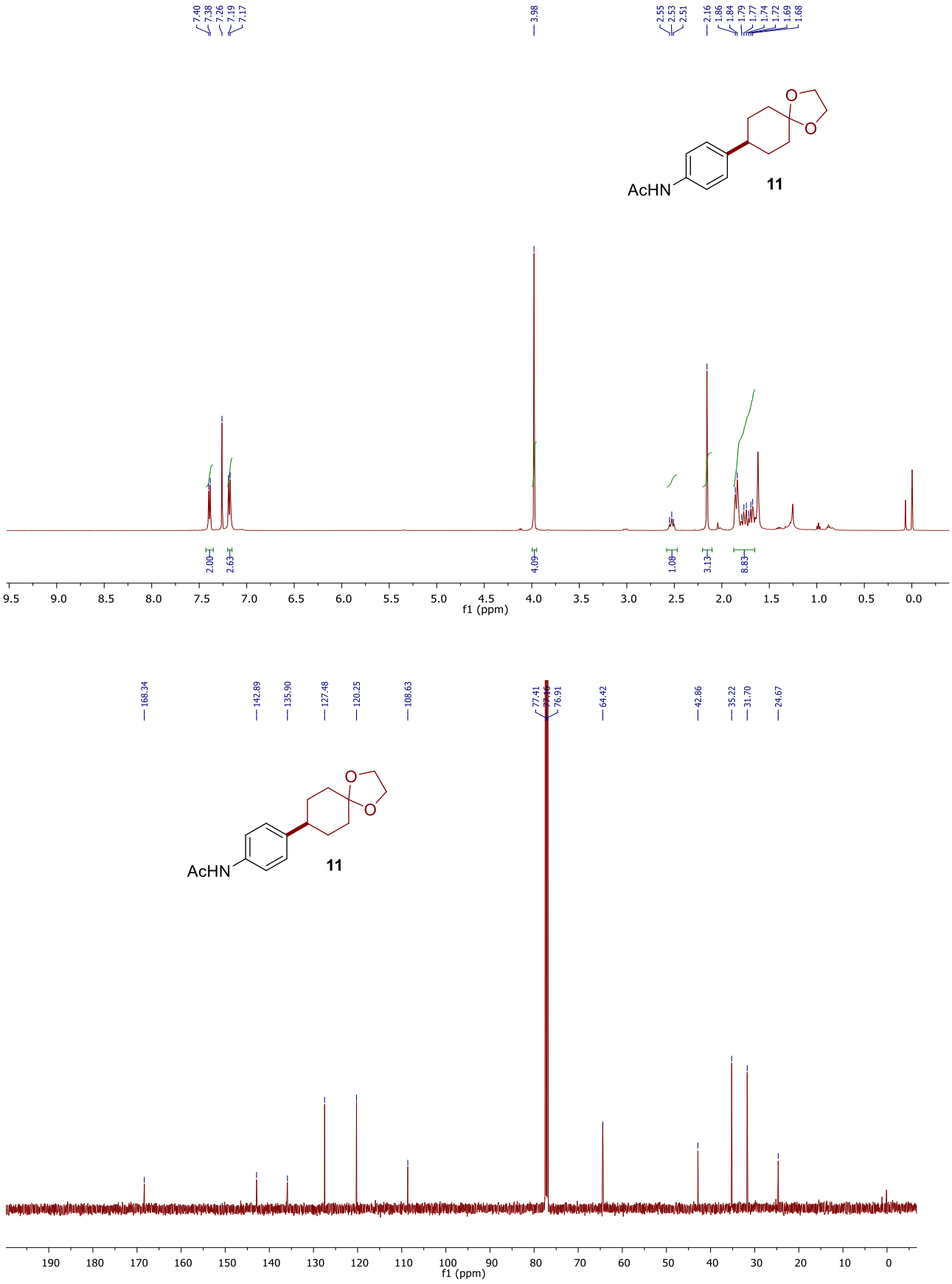

Figure S28. ^{1}H NMR (500 MHz, top) and ^{13}C {1 H} NMR (125 MHz, bottom) Spectra of **11** in $CDCl_3$ at 298K.

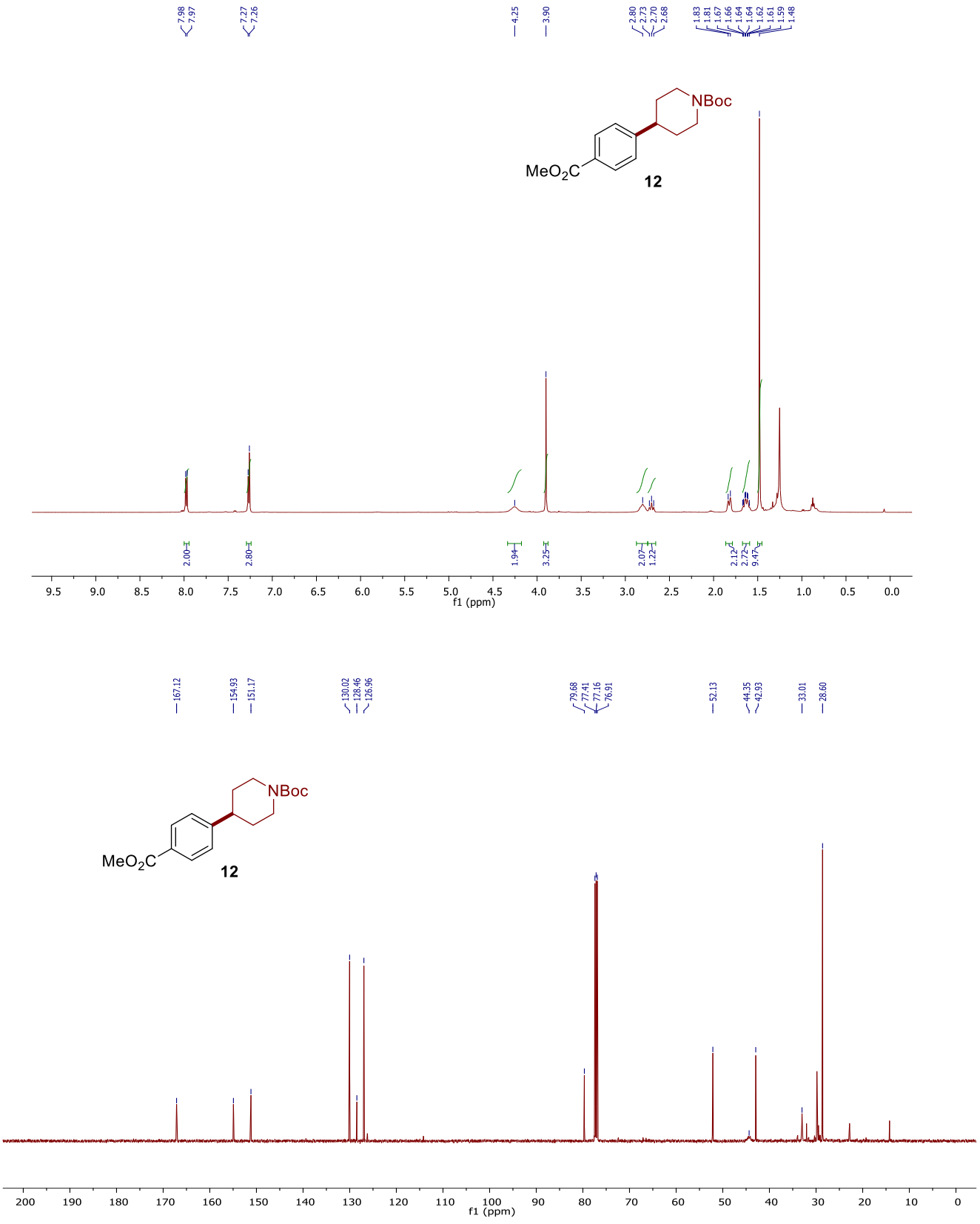

Figure S29. ^{1}H NMR (500 MHz, top) and ^{13}C {1 H} NMR (125 MHz, bottom) Spectra of **12** in $CDCl_3$ at 298K.

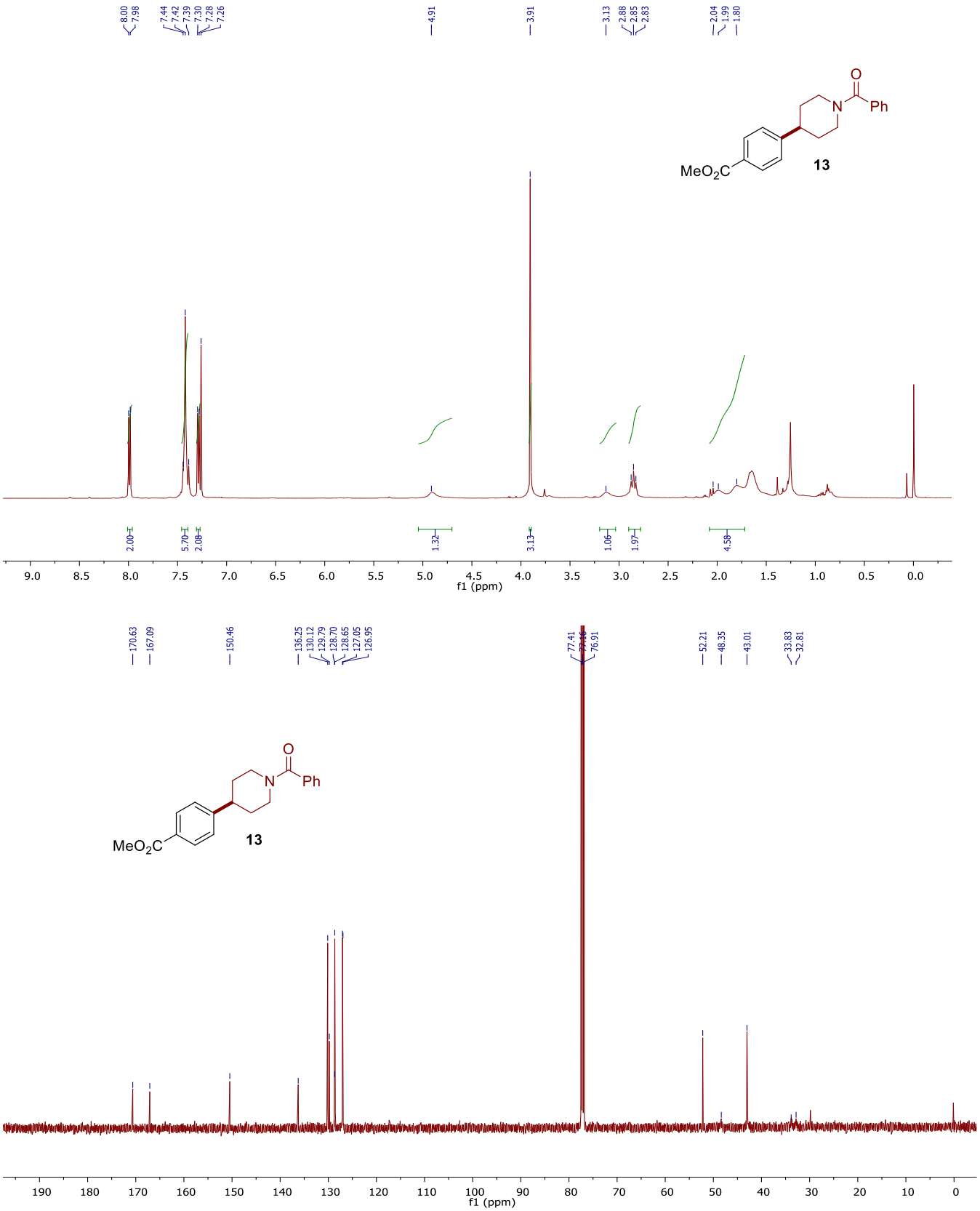

Figure S30. ^{1}H NMR (500 MHz, top) and ^{13}C {1 H} NMR (125 MHz, bottom) Spectra of **13** in $CDCl_3$ at 298K.

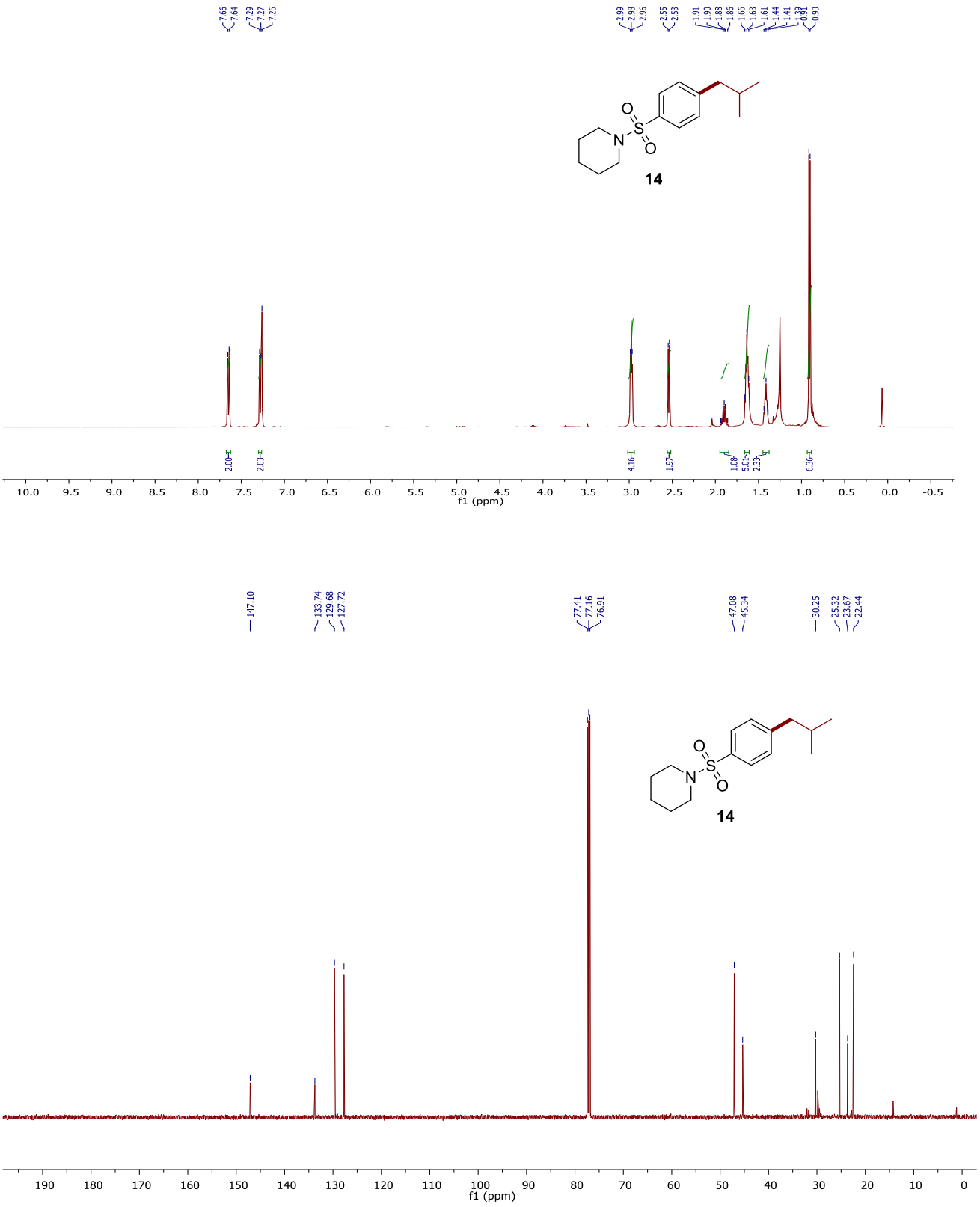

Figure S31. ^{1}H NMR (500 MHz, top) and ^{13}C {1 H} NMR (125 MHz, bottom) Spectra of **14** in $CDCl_3$ at 298K.

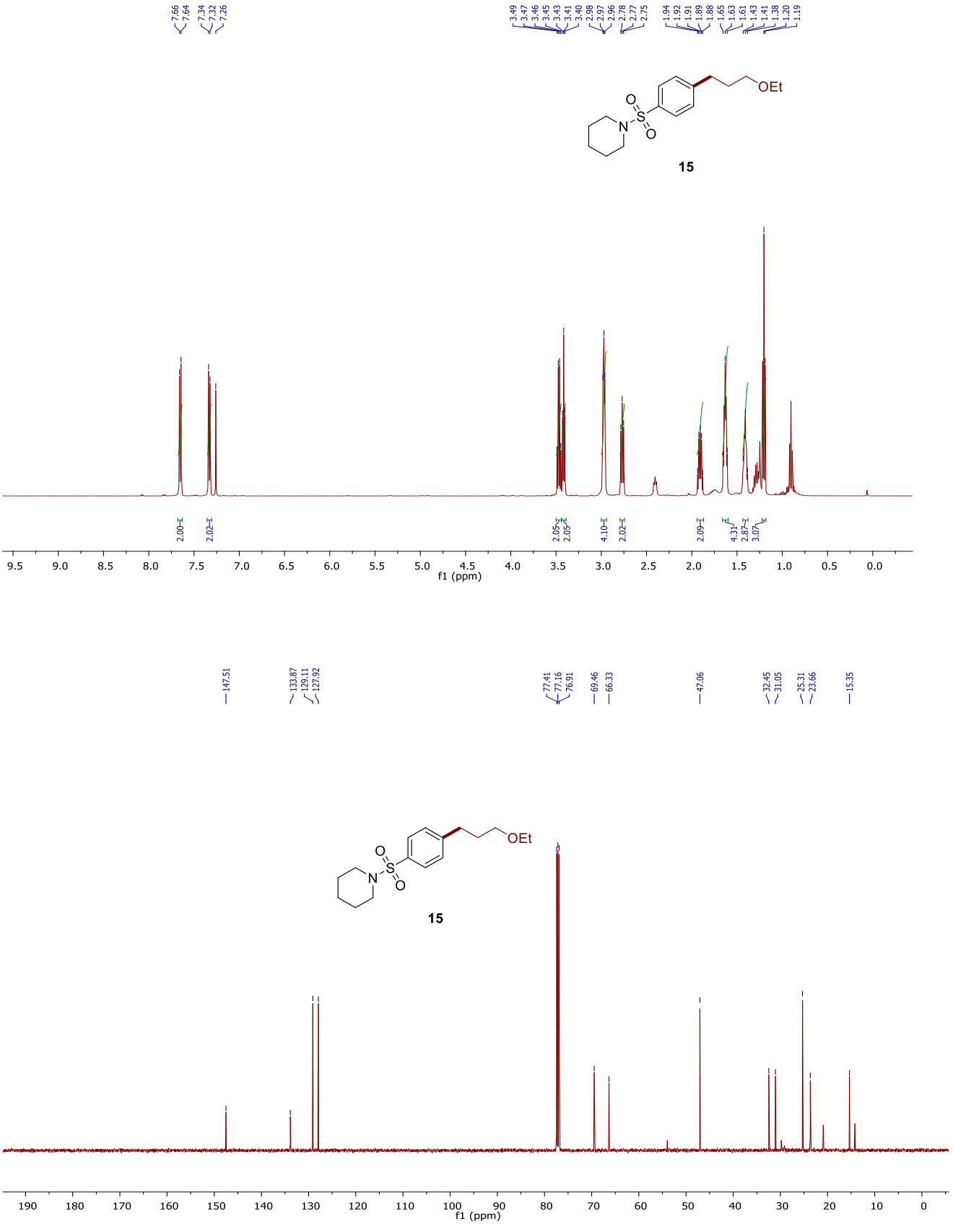

Figure S32. ^{1}H NMR (500 MHz, top) and ^{13}C {1 H} NMR (125 MHz, bottom) Spectra of **15** in $CDCl_3$ at 298K.

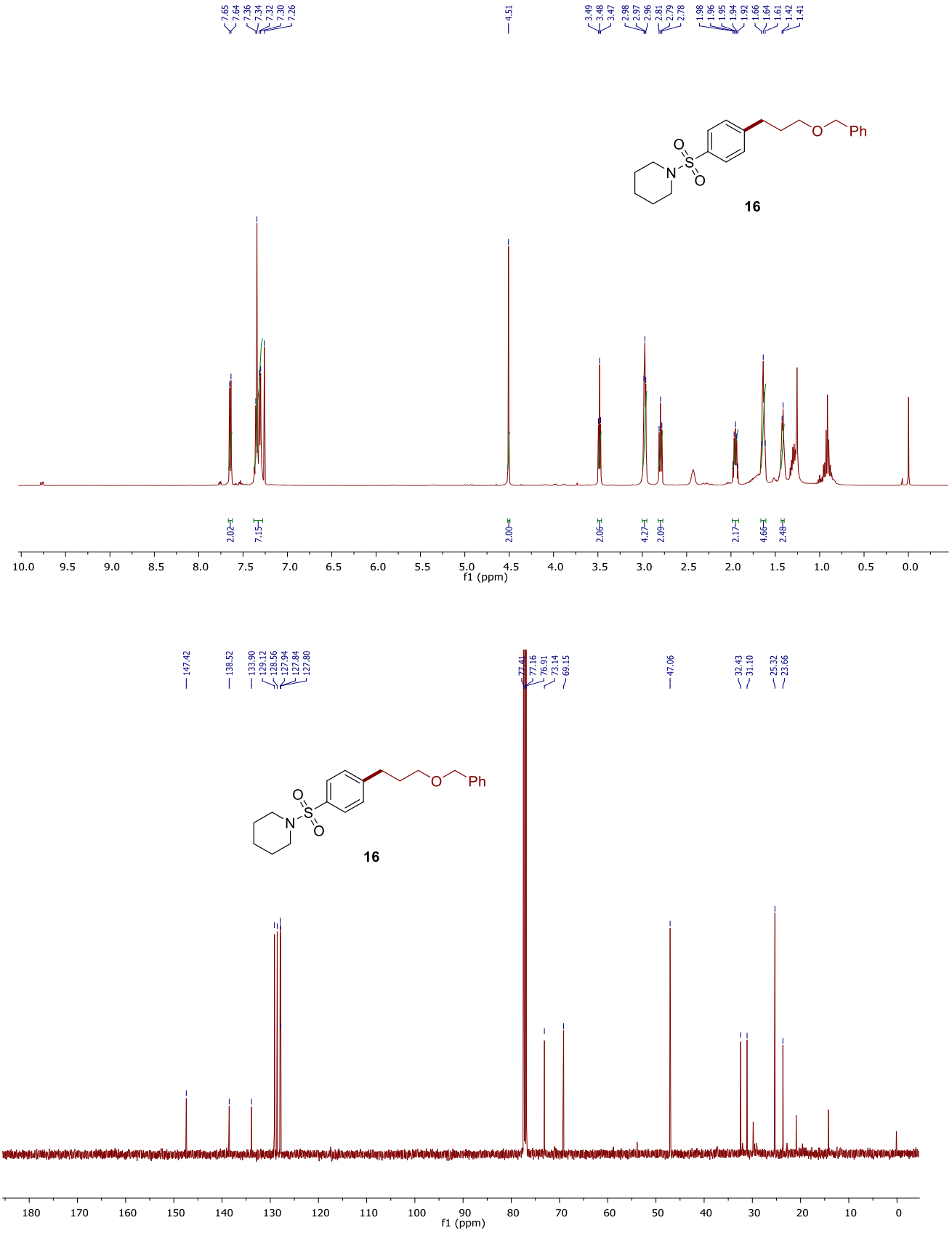

Figure S33. ^{1}H NMR (500 MHz, top) and ^{13}C {1 H} NMR (125 MHz, bottom) Spectra of **16** in $CDCl_3$ at 298K.

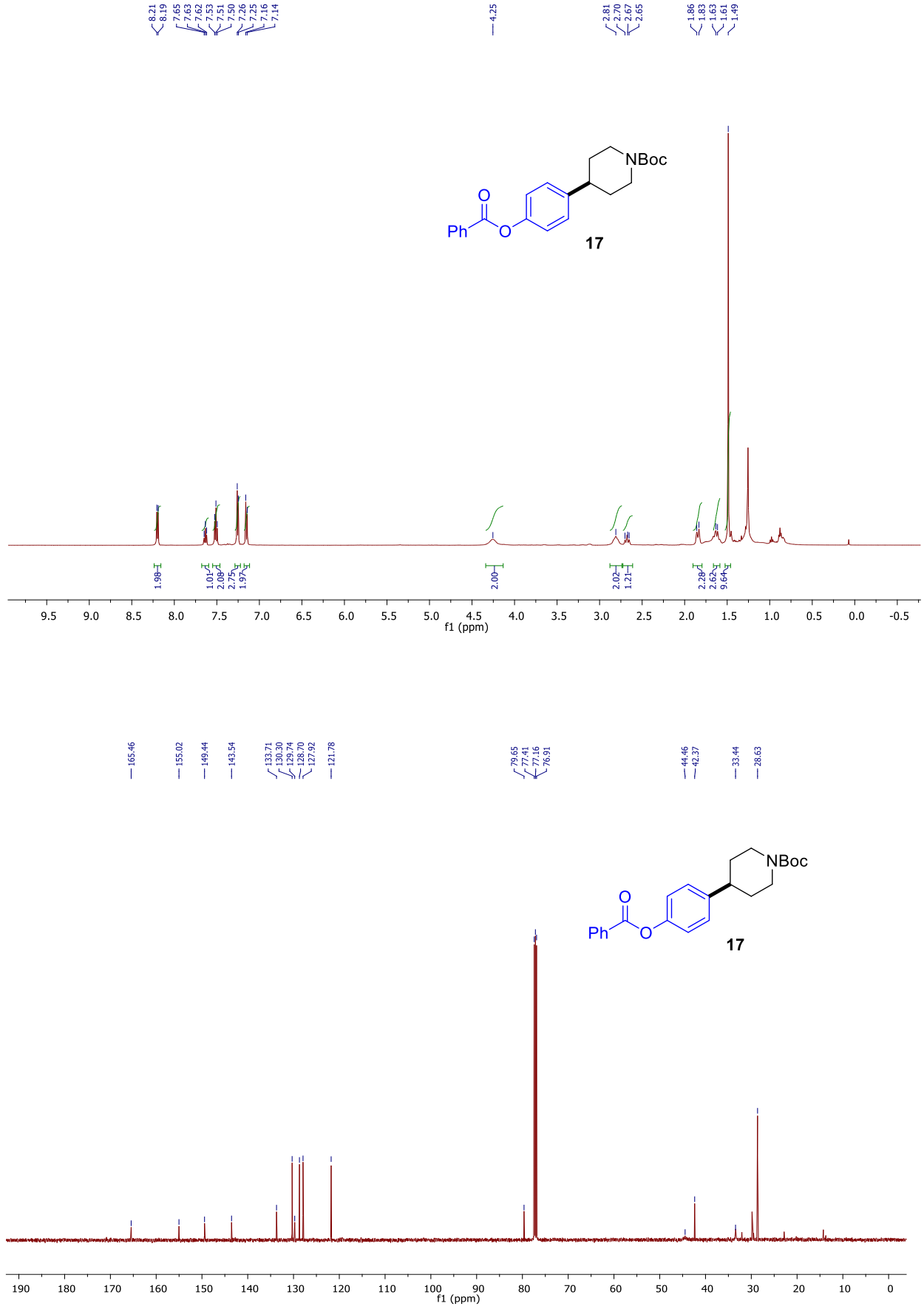

Figure S34. ^{1}H NMR (500 MHz, top) and ^{13}C {1 H} NMR (125 MHz, bottom) Spectra of **17** in $CDCl_3$ at 298K.

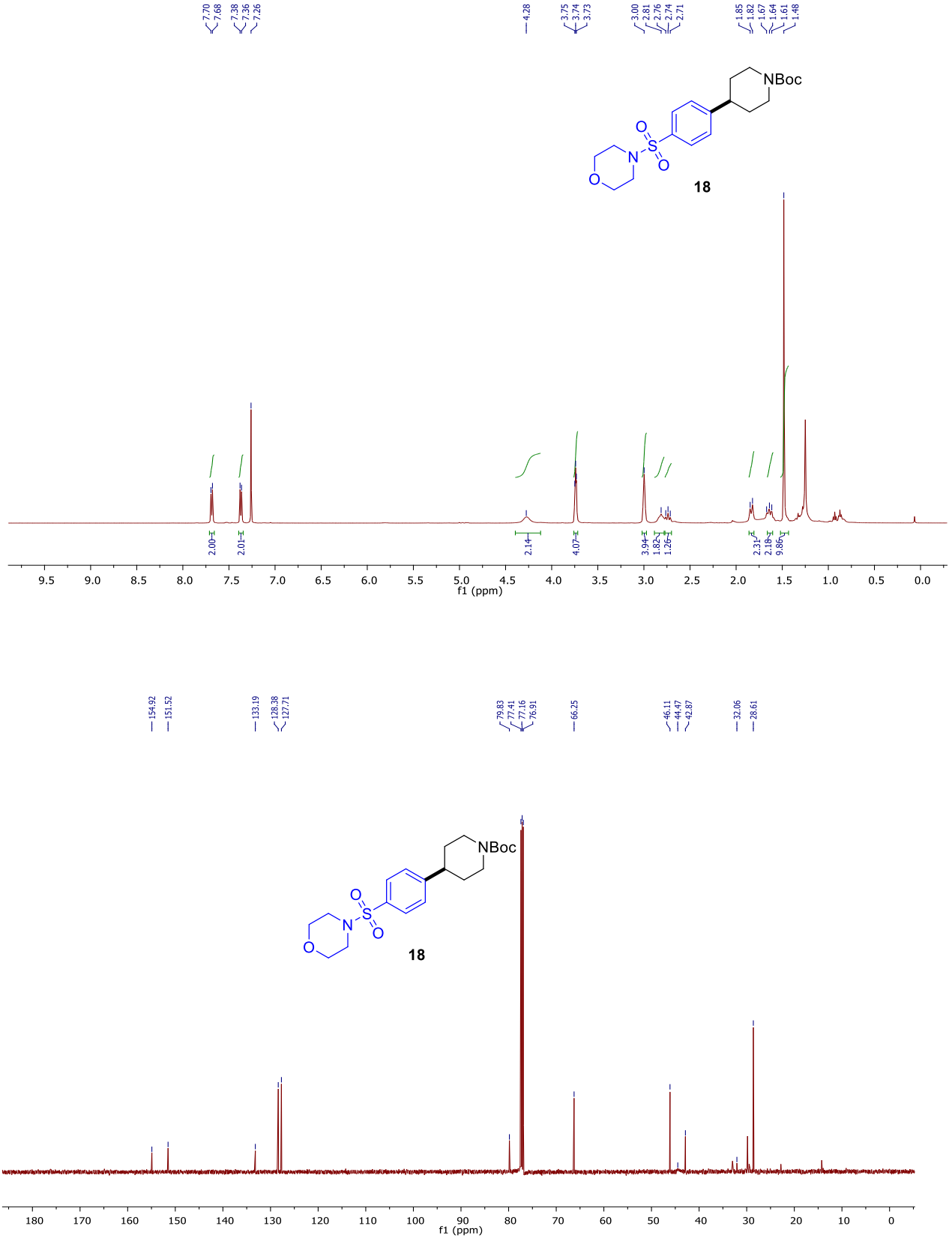

Figure S35. ^{1}H NMR (500 MHz, top) and ^{13}C {1 H} NMR (125 MHz, bottom) Spectra of **18** in $CDCl_3$ at 298K.

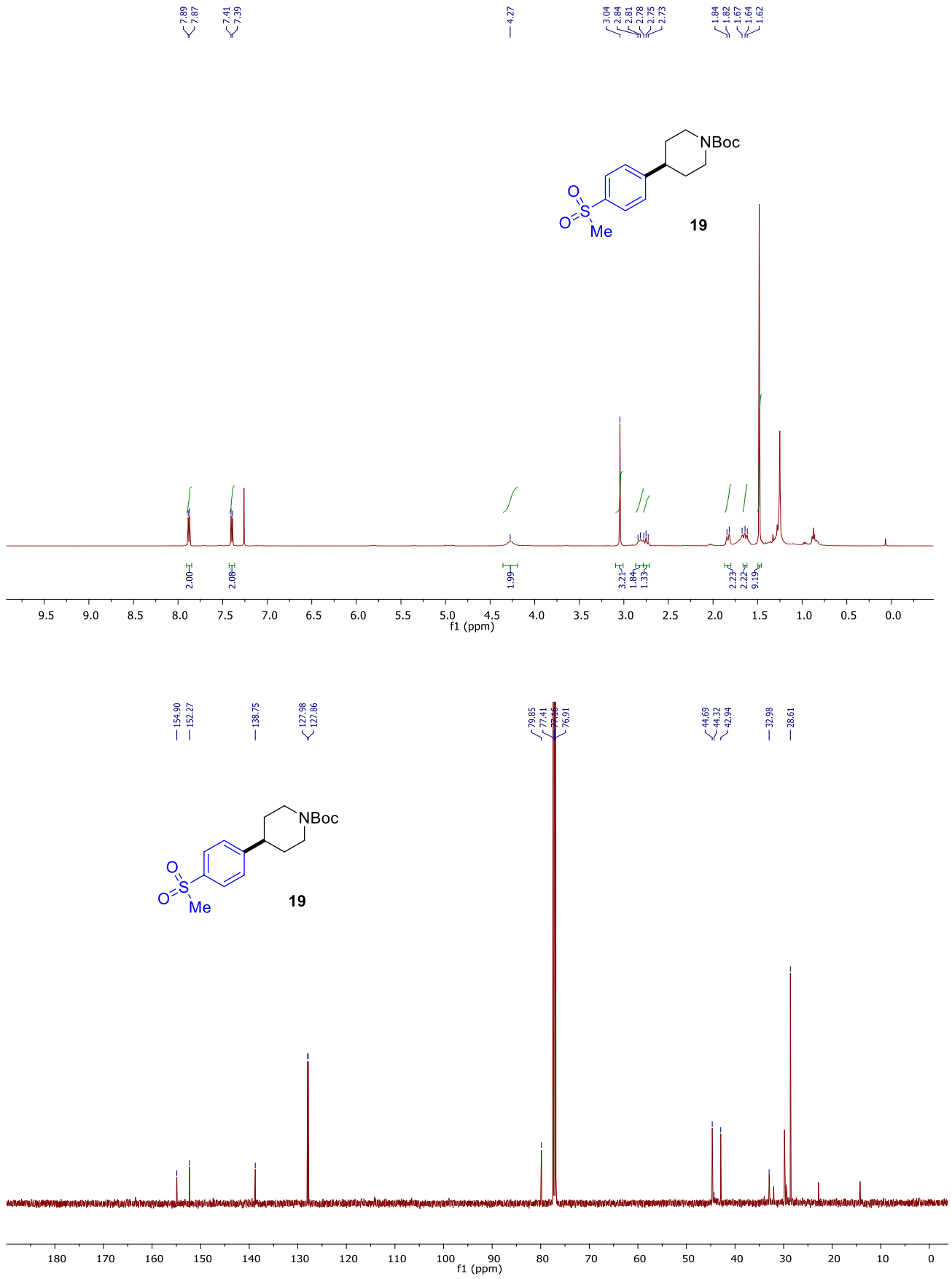

Figure S36. ^{1}H NMR (500 MHz, top) and ^{13}C {1 H} NMR (125 MHz, bottom) Spectra of **19** in $CDCl_3$ at 298K.

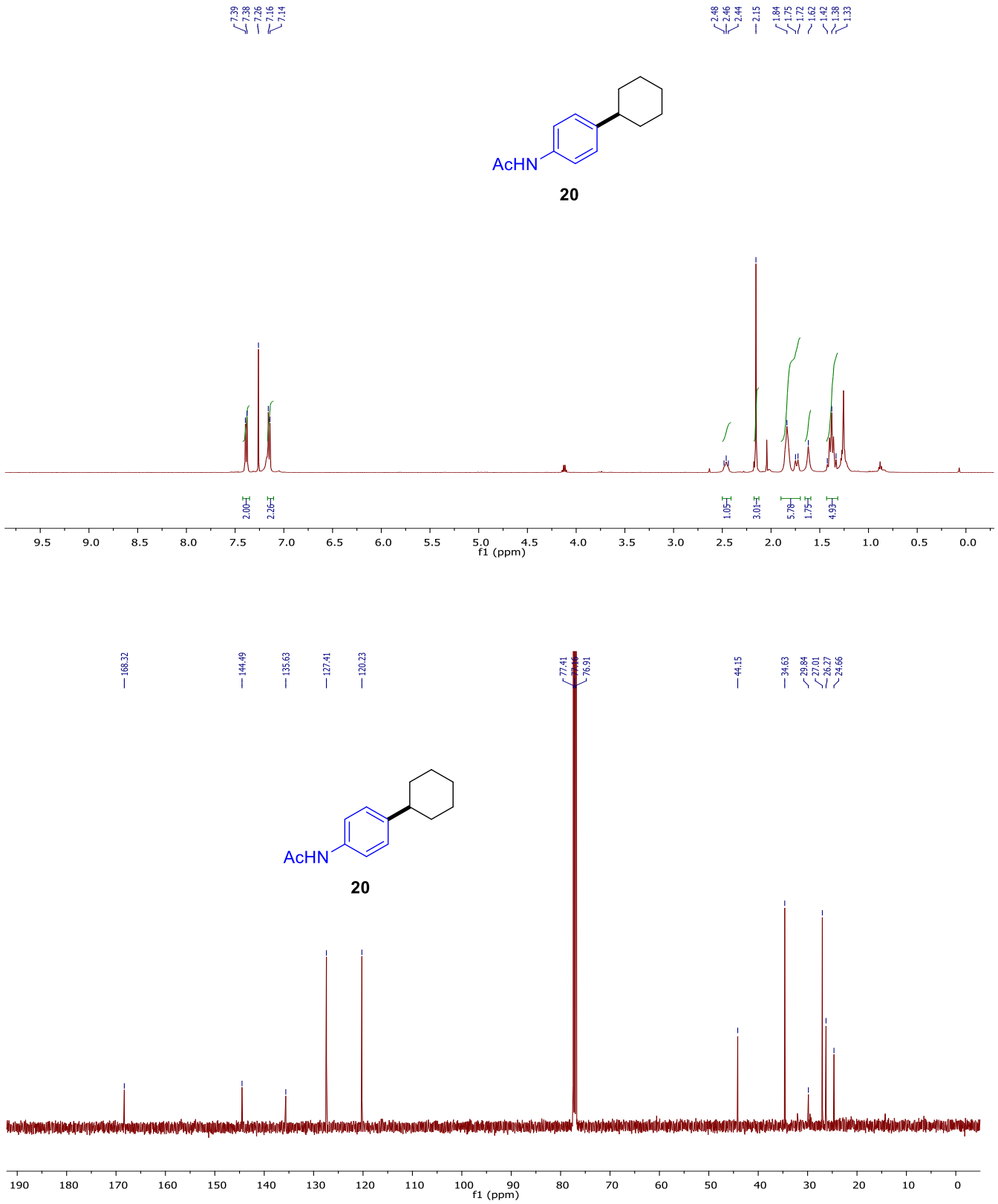

Figure S37. ^{1}H NMR (500 MHz, top) and ^{13}C {1 H} NMR (125 MHz, bottom) Spectra of **20** in $CDCl_3$ at 298K.

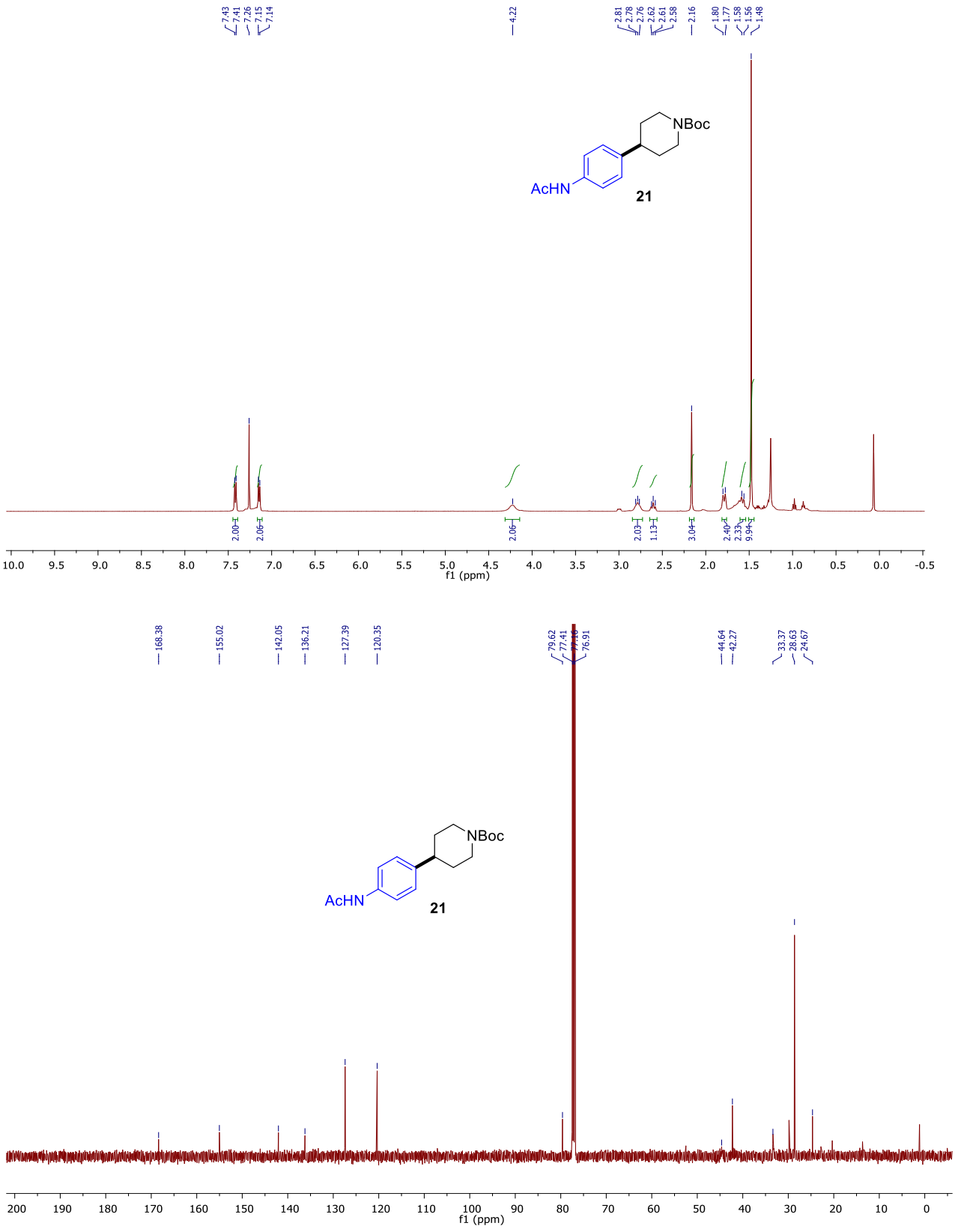

Figure S38. ^{1}H NMR (500 MHz, top) and ^{13}C {1 H} NMR (125 MHz, bottom) Spectra of **21** in $CDCl_3$ at 298K.

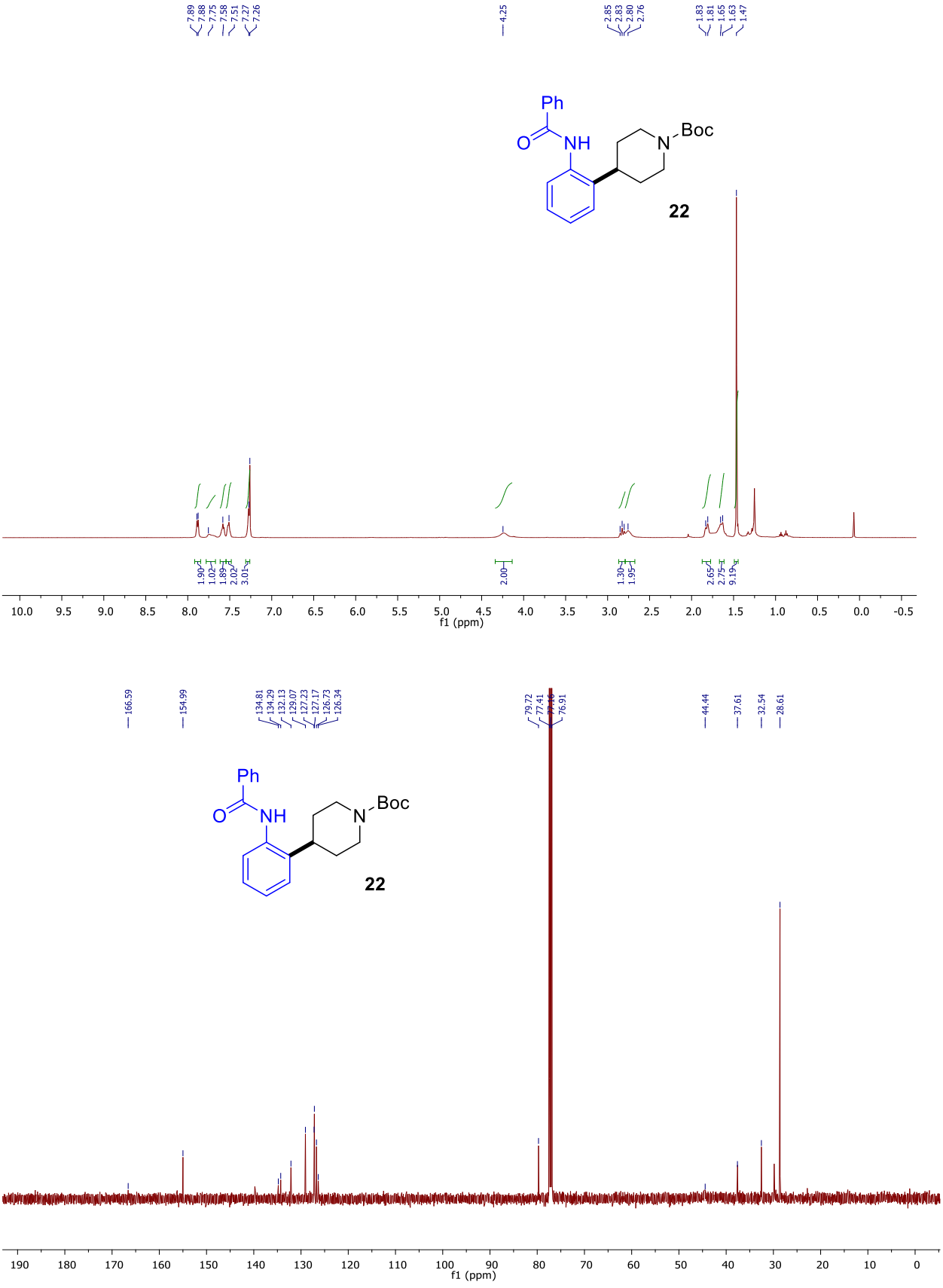

Figure S39. ^{1}H NMR (500 MHz, top) and ^{13}C {1 H} NMR (125 MHz, bottom) Spectra of **22** in $CDCl_3$ at 298K.

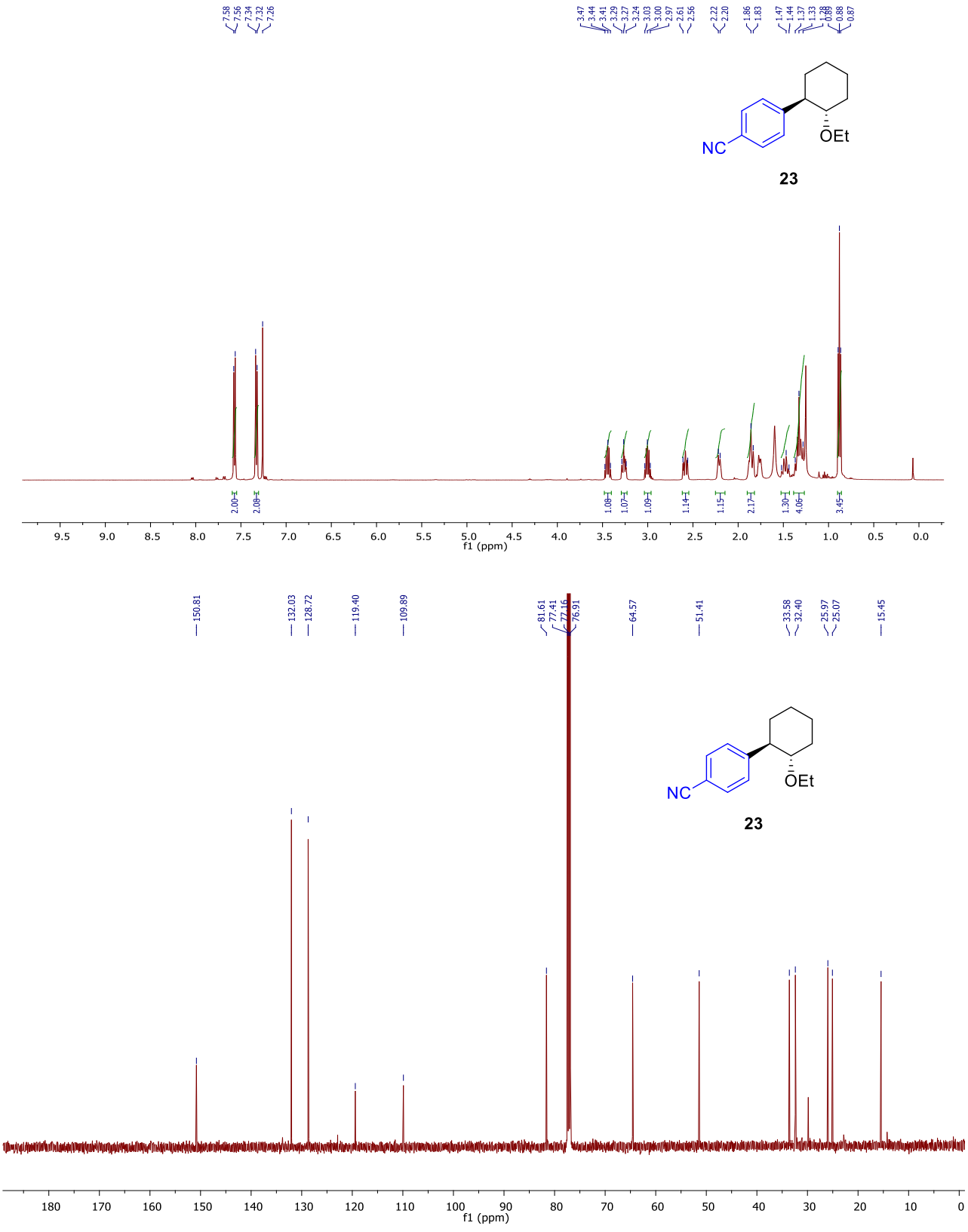

Figure S40. ^{1}H NMR (500 MHz, top) and ^{13}C {1 H} NMR (125 MHz, bottom) Spectra of 2**3** in $CDCl_3$ at 298K.

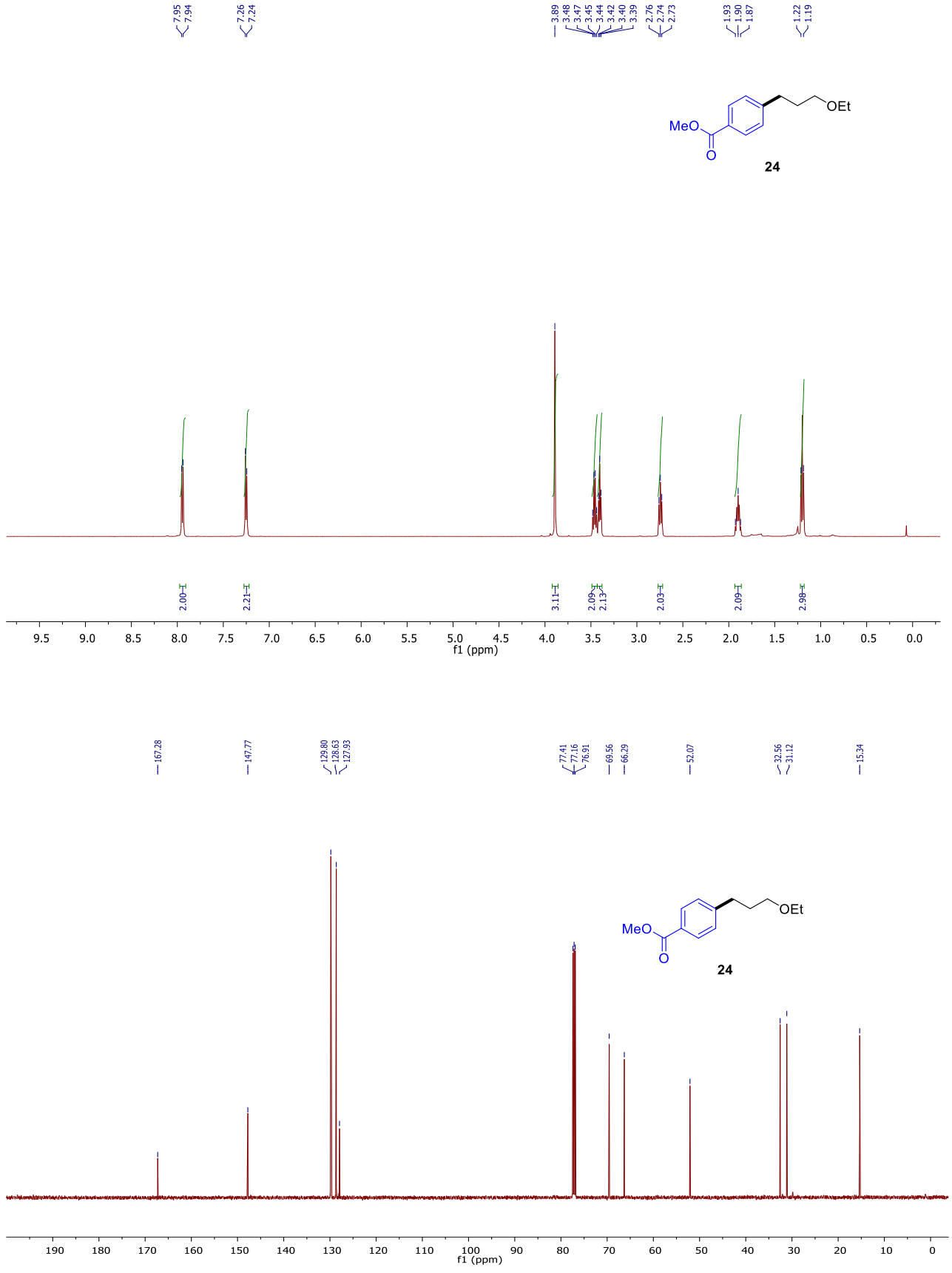

Figure S41. ^{1}H NMR (500 MHz, top) and ^{13}C {1 H} NMR (125 MHz, bottom) Spectra of **24** in $CDCl_3$ at 298K.

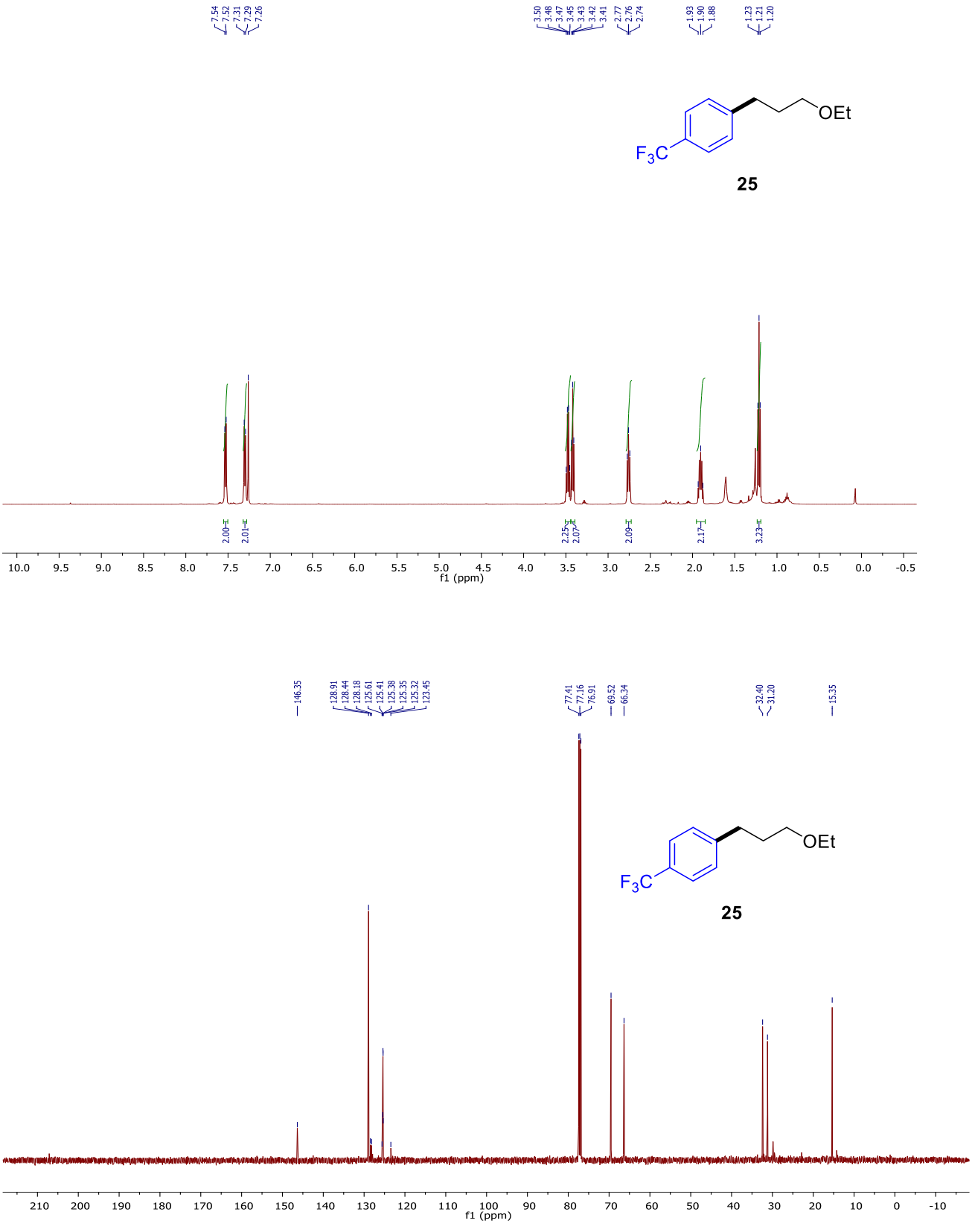

Figure S42. ^{1}H NMR (500 MHz, top) and ^{13}C {1 H} NMR (125 MHz, bottom) Spectra of **25** in $CDCl_3$ at 298K.

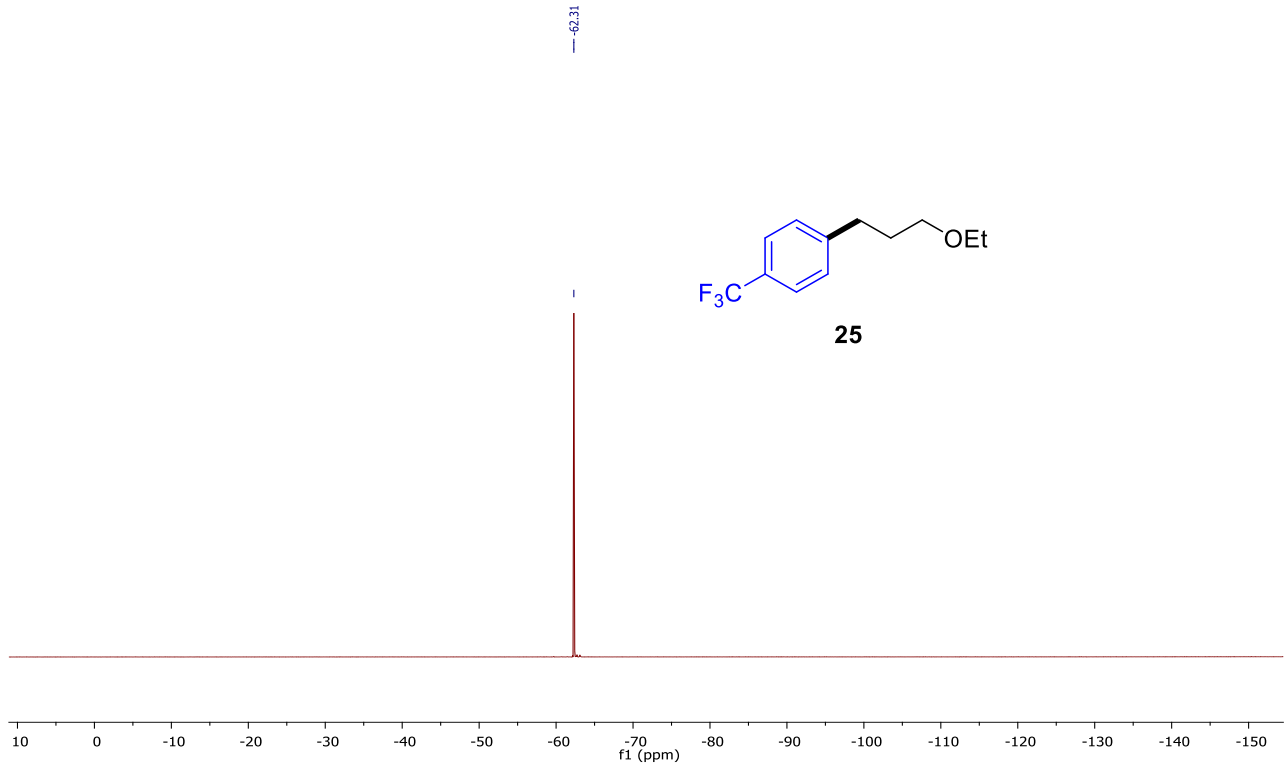

Figure S43. ^{19}FNMR Spectra (471 MHz) of **25** in $CDCl_3$ at 298K.

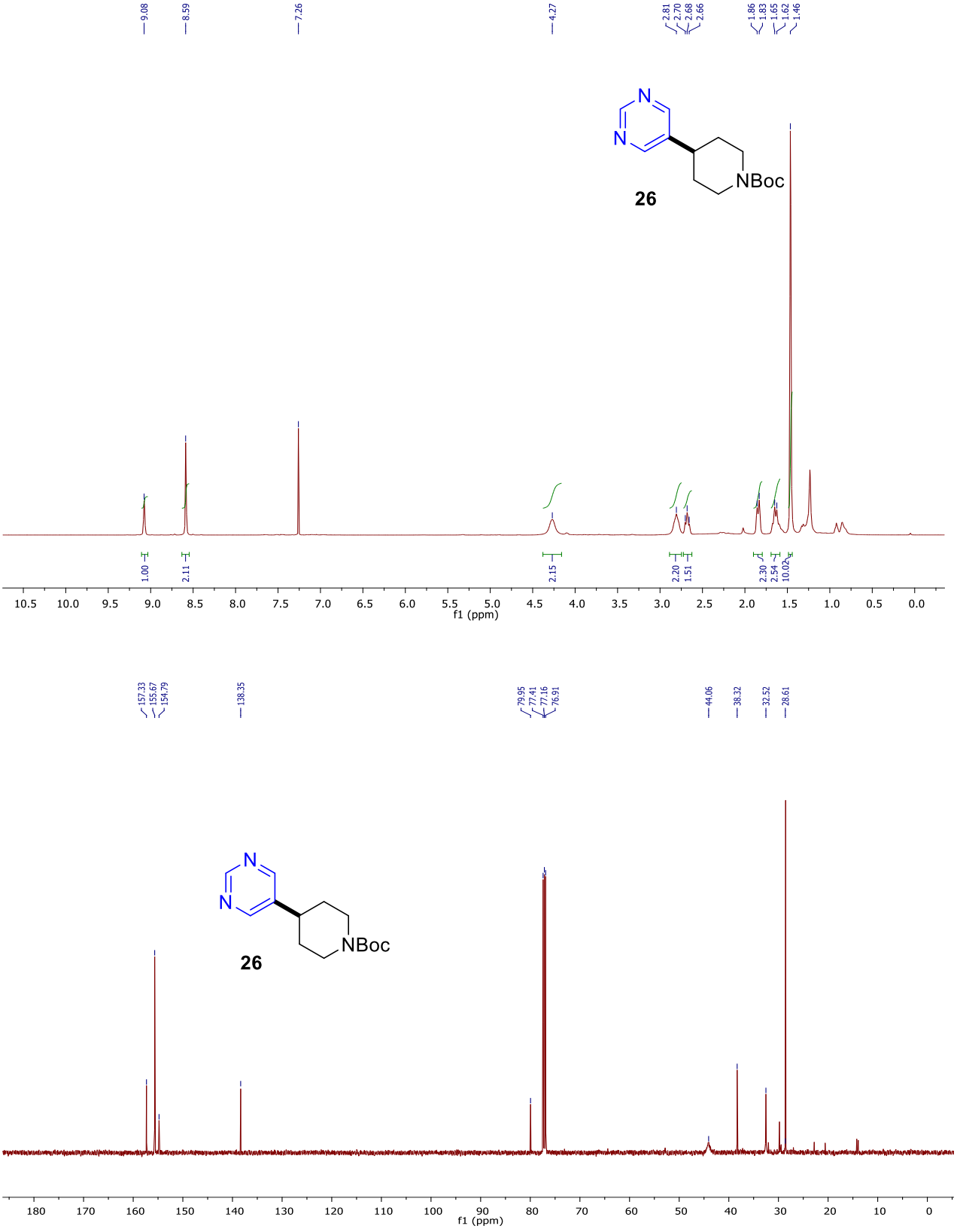

Figure S44. ^{1}H NMR (500 MHz, top) and ^{13}C {1 H} NMR (125 MHz, bottom) Spectra of **26** in $CDCl_3$ at 298K.

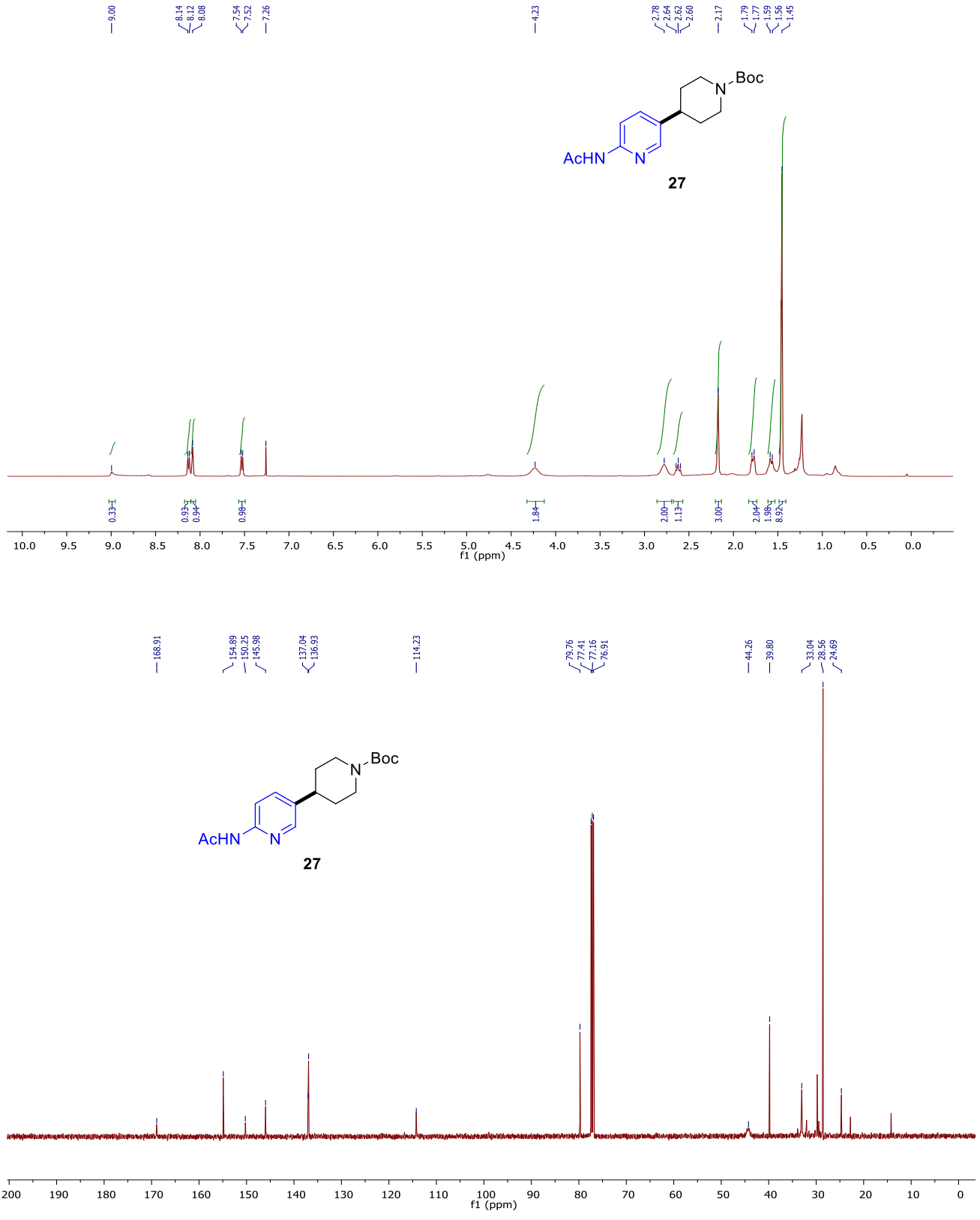

Figure S45. ^{1}H NMR (500 MHz, top) and ^{13}C {1 H} NMR (125 MHz, bottom) Spectra of **27** in $CDCl_3$ at 298K.

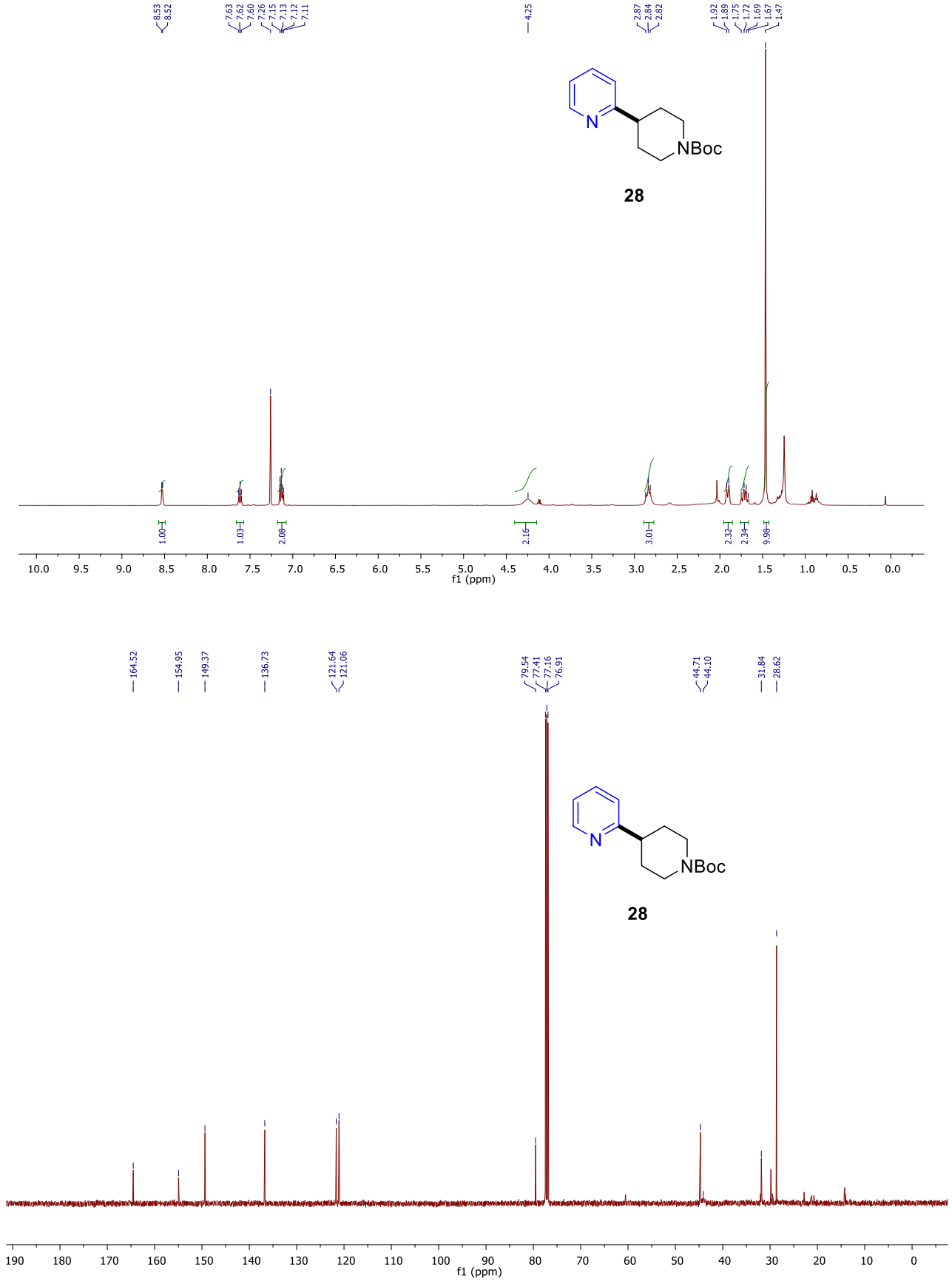

Figure S46. ^{1}H NMR (500 MHz, top) and ^{13}C {1H} NMR (125 MHz, bottom) Spectra of **28** in $CDCl_3$ at 298K.

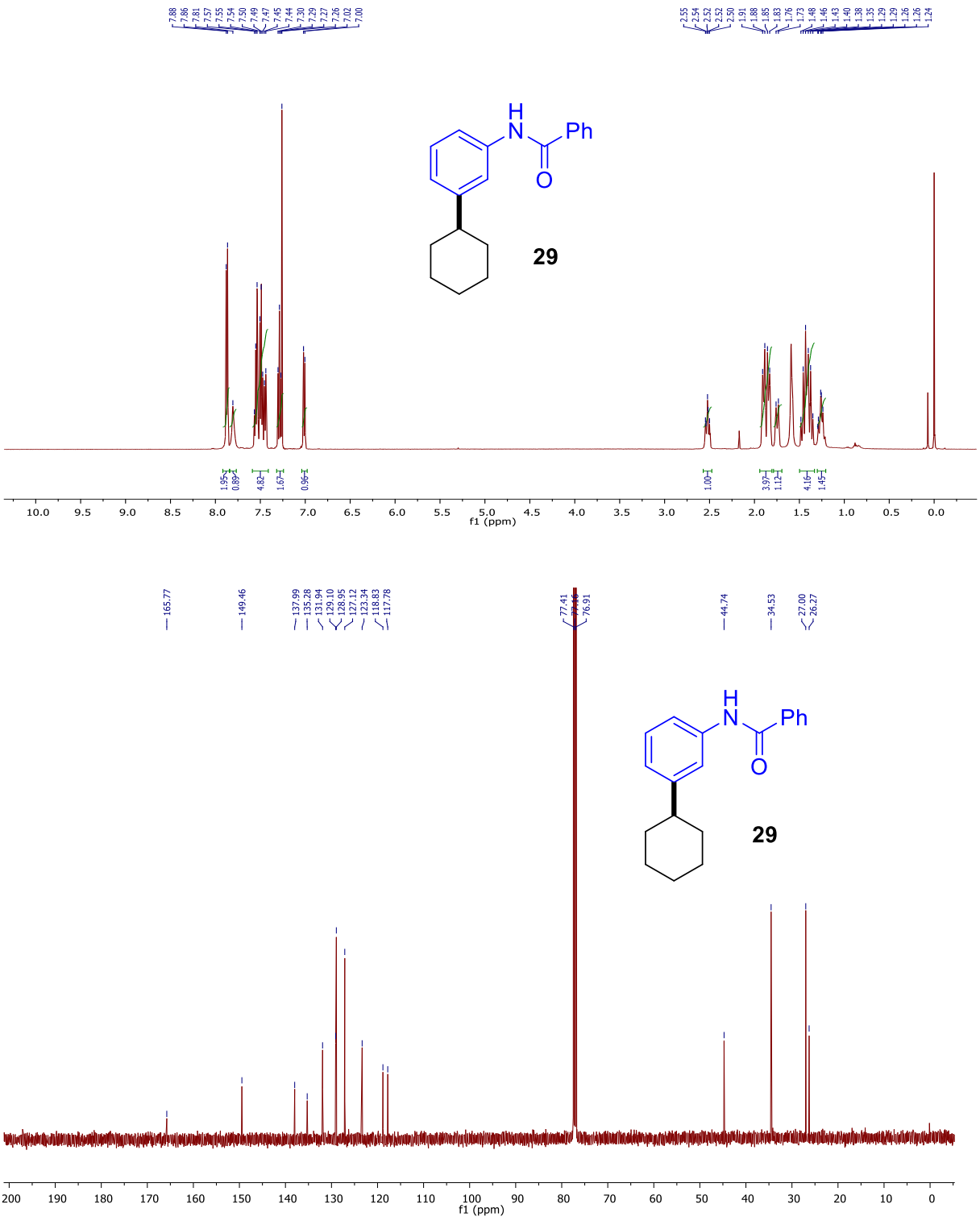

Figure S47. ^{1}H NMR (500 MHz, top) and ^{13}C {1H} NMR (125 MHz, bottom) Spectra of **29** in $CDCl_3$ at 298K.

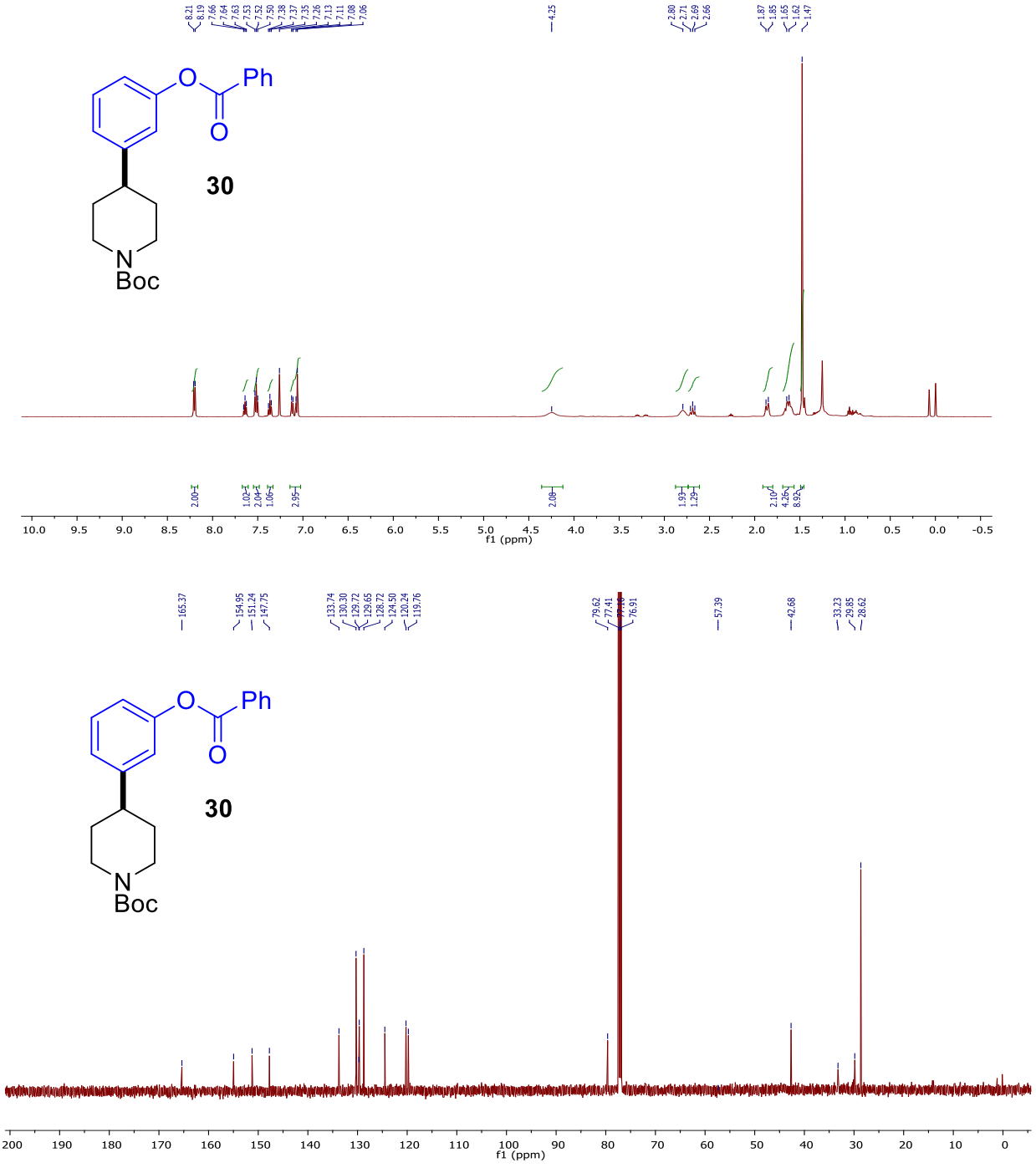

Figure S48. ^{1}H NMR (500 MHz, top) and ^{13}C {1H} NMR (125 MHz, bottom) Spectra of **30** in $CDCl_3$ at 298K.